1971

Apparent and partial molal heat capacities of some aqueous rare earth nitrates and perchlorates from tenth molal to saturation at 25°C

James LeRoy Baker
Iowa State University

Apparent and partial molal heat capacities of some aqueous rare earth nitrates and perchlorates from tenth molal to saturation at 25°C

by

James LeRoy Baker

A Dissertation Submitted to the
Graduate Faculty in Partial Fulfillment of
The Requirements for the Degree of
DOCTOR OF PHILOSOPHY

Major Subject: Physical Chemistry

Approved:

Signature was redacted for privacy.

In Charge of Major Work

Signature was redacted for privacy.

For the Major Department

Signature was redacted for privacy.

For the Graduate College

Iowa State University
Ames, Iowa

1971

TABLE OF CONTENTS

I. INTRODUCTION

Since aqueous solutions of electrolytes play an important part in life processes, man has been interested in these solutions since ancient times. Extensive studies of the behavior of aqueous solutions of electrolytes were conducted in the 19th century. One of the major breakthroughs in these studies was the ionization theory proposed by Arrhenius in 1887 (1). He proposed that in aqueous solutions of electrolytes an equilibrium exists between ions formed by the electrolytic dissociation of solute molecules and undissociated solute molecules. Furthermore, he proposed that the degree of dissociation increased upon dilution and that only in very dilute solution are all the solute molecules completely dissociated. At this same time, van't Hoff (2) discovered that aqueous solutions of electrolytes possess freezing points, boiling points, osmotic pressures, and vapor pressures different from those predicted from equations that are valid for solutions of nonelectrolytes. The realization that these deviations are due to the dissociation of electrolytes into ions provided striking evidence for Arrhenius' theory.

Although Arrhenius' ionization theory works quite well for dilute solutions of weak electrolytes, it has several flaws when solutions of strong electrolytes are considered. Contrary to the theory, strong electrolytes are 100% dissociated even at finite concentrations. Another flaw

is the failure of the theory to explain the fact that ionic mobilities and dissociation constants are concentration dependent.

One of the deficiencies of the simple ionization theory is its lack of consideration of the electrostatic forces between charged particles in solution. In 1912, Milner (3) made an attempt at predicting the effects of ionic interactions on the behavior of very dilute solutions. His treatment has since been described as excellent, but at the time it involved laborious numerical calculations and was not widely understood.

For the most part, other attempts were unsuccessful until 1923 when Debye and Hückel (4) derived their now famous theory which relates the electrical free energy of a solution to its concentration. In order to derive their theory, Debye and Hückel assumed that the solute is completely dissociated into ions. They also had to make other simplifying assumptions which are only valid for a concentration range in the very dilute region. For example, they assumed that ion-solvent interactions do not change with concentration, and that the departure of solutions from ideal behavior is due solely to the long-range electrostatic interactions of the ions. Since 1923, an impressive array of experimental evidence has been collected demonstrating the validity of the Debye-Hückel theory for very dilute solutions. However, attempts to extend

this theory to concentrated solutions, which are of more practical interest, have failed.

Concentrated solutions are much more complex than very dilute solutions. There are, in addition to the long-range electrostatic interactions between ions, short-range ion-ion interactions that may result in ion association such as the formation of complexes or water-separated ion pairs. There are also concentration dependent ion-water interactions which involve the formation of hydrates and hydrolysis products. Furthermore, changing ion-water interactions result in changes in the water-water interactions as they occur in pure liquid water. Because the water-water interactions, i.e., hydrogen-bonding, in pure liquid water result in the formation of a constantly rearranging three-dimensional network of associated molecules, water itself is one of the most complex substances known to man. Its structure is still a matter of great controversy. Since there are even more interactions in concentrated solutions, no simple theory can predict the behavior of these solutions. Even after many years of research there are no adequate theories for concentrated aqueous solutions of electrolytes.

There are various ideas on the best possible method of obtaining an adequate theory. It is the belief of Harned and Owen (5) that extension of present theory cannot solve the problem of predicting the behavior of concentrated solutions.

Fuoss and Onsager (6) suggest that the theory of concentrated solutions should be approached with an adequate theory of fused salts. Whatever theories that may be derived in the future will have to take into account ion-ion, ion-water, and water-water interactions that occur in solution. Therefore, in order to predict the behavior of concentrated solutions, it will be necessary to have a knowledge of the microscopic structure of solutions and be able to correlate this structure with the macroscopic properties.

There are two approaches that can be used to attack the problem of understanding solution phenomenon. In the first approach models for the solution on a microscopic level are developed assuming certain interactions are occurring, and then using statistical mechanics, values for the macroscopic properties are calculated. How closely these values agree with the experimentally determined values is the criteria used to judge the accuracy of the model's interpretation of the microscopic structure of solution.

In the second approach values for many macroscopic properties of solutions are experimentally determined as a function of concentration, temperature, and pressure. Since the macroscopic properties are statistical averages of very large numbers of atomic level occurrences, it is rarely possible to proceed with certainty from one macroscopic property to microscopic behavior. However, if a comparison of many macroscopic

properties for a given system is made, it is often possible to draw conclusions as to the presence or absence of certain interactions.

It is apparent that a certain amount of work utilizing the second approach must be performed before the first approach can be useful. The first approach requires experimental data with which to compare the calculated quantities, and in order to develop a realistic model for the solution, there must be some ideas as to possible interactions in solutions. Since there is little data in the literature on the macroscopic properties of solutions which contain polyvalent ions, the second approach was used in this laboratory for the three to one charge type electrolytes. Because many interactions in solution are enhanced by the higher charged ions, the properties of aqueous solutions containing polyvalent ions are of interest. An extensive program was initiated in this laboratory in the 1950's to determine the thermodynamic and transport properties of rare earth chloride, nitrate, and perchlorate solutions. Since then spectroscopic and structural studies of these solutions have also been initiated.

The rare earths, which have become available in kilogram quantities because of large scale ion exchange processes developed at Ames Laboratory (7), provide an excellent series to study from both experimental and theoretical standpoints. The rare earths of interest (elements 57 through 71) all form

the trivalent cations in solution and exhibit very similar chemical behavior. The similarity of the rare earths is due to their unique electronic configurations. As the atomic number increases across the series the additional electrons are added to the 4f subshell starting with La, which has no 4f electrons, and ending with Lu, which has a filled subshell of fourteen 4f electrons. The 4f subshell is shielded by the filled 5s and 5p subshells, and therefore the 4f electrons have little influence on the chemical properties of the rare earths. The increase in nuclear charge across the series does cause a regular decrease in the ionic radius of the trivalent cations; the decrease is from 1.061 Å for La to 0.848 Å for Lu as reported by Templeton and Dauben (8) and causes a corresponding increase in the charge density of the trivalent cations. The rare earths then provide an opportunity to study the effect of ionic size and charge density on solution properties.

Because the rare earths form a number of highly water-soluble salts, their solutions can be studied over a wide concentration range. The very soluble salts can be used to study systems approaching fused salts, e.g., $Yb(NO_3)_3$ and $Lu(NO_3)_3$ which are soluble to concentrations in excess of 6.6 molal. Advantages of the rare earths relative to other trivalent cations are that their degree of hydrolysis is small and in dilute solutions their tendency to form complexes is generally slight. This enables the effect of the hydration

of the highly charged rare earth ions to be studied.

By varying the anion, information can be obtained on the effects of anion size as well as the degree of complexation on the properties of solutions. The perchlorate ion is of interest because of its effect on the structure of water, and because it does not readily form complexes with cations. The nitrate ion, however, generally does form complexes with polyvalent cations. The chloride ion falls between the perchlorate ion and the nitrate ion in its degree of complexing and may form hydrogen-bonds with water in solution.

One of the thermodynamic properties of solutions that is of interest is the heat capacity. It is well known that the heat capacity of a given amount of water is greater than the heat capacity of that water after the addition of a small amount of strong electrolyte. This has been explained in terms of the effect the ions have on the structure of the solvent causing the heat capacity of the water to decrease by an amount greater than the intrinsic heat capacity of the ions. The heat capacities of dilute solutions should then provide information on ion-water interactions. At higher concentrations the amount of complexing taking place between the cation and anion, if any, should increase and result in changes in the heat capacities of the solutions.

This thesis is a report of the specific heat capacities of aqueous solutions of Pr, Sm, Tb, Dy, Ho, Tm, and Yb nitrate and Pr, Sm, Tb, Dy, Ho, Er, Tm, and Yb perchlorate determined as a function of concentration from 0.1 molal to saturation at 25°C. From the specific heat capacities, apparent molal heat capacities for each salt were calculated and fit to an analytic function of concentration with the aid of a computer. The partial molal heat capacities of the solute and solvent were then calculated from this function.

Studies of apparent molal volumes (9,10,11), apparent molal heat contents, (12,13), and apparent molal heat capacities (14,15,16) for the rare earth chlorides have indicated that the rare earths are divided into two series with different coordination numbers. The rare earths Sm, Eu, and Gd fall between the two series and are assumed to exist in solution as equilibrium mixtures of the two coordination types. It was interesting to see if this behavior was also indicated in the apparent molal heat capacity data for the rare earth perchlorates determined in this work and by Walters (16). Raman and infrared spectral evidence (17,18,19,20) has indicated that the perchlorate anion is unique in its effect on the structure of water. Therefore, heat capacity data on perchlorate solutions were of interest.

Studies of the apparent molal volumes (9,11) and apparent molal heat contents (21) of rare earth nitrates have

indicated that complexes are forming even in dilute solutions. The trend associated with the change in coordination across the rare earth series is observed for apparent molal volumes at infinite dilution. However, at concentrations of a few thousandths molal the trend is becoming obscurred due to complexation between the cation and anion. This study sought to determine how the heat capacity data for the rare earth nitrates determined in this work and by Walters (16) correlated with the other properties of solutions.

Heat capacity data alone do not furnish a complete understanding of solution phenomenon. These data do, however, contribute to that understanding and should provide a stringent test for any theories derived in the future. In addition, partial molal heat capacities determined in this work are of practical value in calculating the temperature dependence of heats of dilution and activities for the rare earth salt solutions.

II. THERMODYNAMIC INTRODUCTION

A. Definitions and Basic Concepts

Thermodynamics is one of the most powerful tools of physical chemistry. It provides exact relationships between macroscopic properties of a system in an equilibrium state and also relationships between properties of a system in different equilibrium states. For example, the difference in energy, ΔE, for a system of constant mass in two different states is given by the first law of thermodynamics

$$\Delta E = E_2 - E_1 = Q + W \qquad (2.1)$$

where by convention, in passing from state 1 to state 2, Q is the heat absorbed by the system and W is the work done on the system. Because the energy, E, is dependent only on the state of the system and not on the system's previous history, ΔE is dependent only on states 1 and 2 and not on the route between them. This is not the case with Q and W as they are interrelated, and their values depend on the route by which state 1 passes to state 2. Therefore, when discussing two states that differ in energy, in order to know how much heat, Q, was absorbed, the route between states must be specified, likewise for the work, W.

In addition to energy, another function of interest is enthalpy, H, which is defined by

$$H = E + PV$$

The change in enthalpy with a change in state is

$$\Delta H = \Delta E + \Delta(PV) \tag{2.2}$$

If a process is specified in which only pressure-volume work is done and the pressure is held constant, Equations 2.1 and 2.2 become respectively

$$\Delta E = Q_p - P\Delta V$$

$$\Delta H = \Delta E + P\Delta V$$

which when combined yield

$$\Delta H = Q_p \tag{2.3}$$

Therefore, Equation 2.3 shows that the heat absorbed in a process at constant pressure is equal to the change in enthalpy if only pressure-volume work is done.

The average heat capacity of a system at constant pressure in the temperature interval Θ_1 to Θ_2 is

$$C_{p\ avg} = \frac{Q_p}{\Theta_2 - \Theta_1} = \frac{\Delta H}{\Theta_2 - \Theta_1} \tag{2.4}$$

Because the heat capacity of a system is dependent on temperature, the true heat capacity of a system at constant pressure and a given temperature Θ_1 is

$$C_p = \lim_{(\theta_2 \to \theta_1)} \frac{Q_p}{\theta_2 - \theta_1} = \frac{dQ_p}{d\theta}$$

However, in many cases including this work the difference between the true heat capacity and the average heat capacity as defined by Equation 2.4 is negligible compared to experimental error when the temperature difference, $\theta_2 - \theta_1$, is of the order of a degree. The temperature difference employed in this work was 1.2°C, and Equation 2.4 was used as the operational definition for heat capacity at constant pressure. The measure of heat capacity used in this work was specific heat capacity which is defined as the heat capacity of a system per unit mass.

B. Apparent and Partial Molal Quantities

It is convenient to distinguish between two types of properties: 1) those dependent on the amount of matter in a system, and 2) those independent. Properties such as temperature, pressure, and specific heat capacity are independent of mass and are called intensive properties. Properties such as volume and heat capacity are dependent on the mass and are called extensive properties. Since extensive properties are proportional to the mass or, in other words, are homogeneous functions of degree one, Euler's theorem may be used.

For an extensive property J, which is a function of the number of moles, n_1 and n_2, of components 1 and 2 in a binary system, Euler's theorem states

$$J(n_1,n_2) = n_1\left(\frac{\partial J}{\partial n_1}\right)_{n_2} + n_2\left(\frac{\partial J}{\partial n_2}\right)_{n_1} \qquad (2.5)$$

By definition, the partial derivatives in Equation 2.5 are the partial molal property J for component 1 and component 2, respectively. Partial molal quantities are independent of the amount of matter in a system and are therefore intensive properties; they are, however, dependent on the composition of the system.

Considering in particular the heat capacity of aqueous electrolyte solutions, $C_p(n_1,n_2,T,P)$, at constant temperature and pressure, Equation 2.5 becomes

$$C_p = n_1\left(\frac{\partial C_p}{\partial n_1}\right)_{n_2,T,P} + n_2\left(\frac{\partial C_p}{\partial n_2}\right)_{n_1,T,P} \qquad (2.6)$$

where C_p is the heat capacity of the solution, n_1 is the number of moles of water, and n_2 is the number of moles of solute in the solution. Equation 2.6 becomes

$$C_p = n_1\overline{C}_{p1} + n_2\overline{C}_{p2} \qquad (2.7)$$

upon introduction of the symbols $\overline{C}_{p1}$ and $\overline{C}_{p2}$ where $\overline{C}_{p1}$ is the partial molal heat capacity of water, and $\overline{C}_{p2}$ is the partial molal heat capacity of the solute.

Physically $\overline{C}_{p1}$ is defined as the change in the heat capacity of an infinite amount of solution with the addition of one mole of water, similarly for $\overline{C}_{p2}$ and the solute. Because direct measurement of the partial molal heat capacities is impracticable, the quantity Φ_{cp} is defined

$$\Phi_{cp} = \frac{C_p - n_1\overline{C}_{p1}^{\circ}}{n_2} \tag{2.8}$$

where $\overline{C}_{p1}^{\circ}$ is the heat capacity per mole of pure water. Rearranging Equation 2.8 and differentiating with respect to n_2 at constant n_1, constant temperature, and constant pressure results in the expression for $\overline{C}_{p2}$

$$\left(\frac{\partial C_p}{\partial n_2}\right)_{n_1,T,P} = \overline{C}_{p2} = \Phi_{cp} + n_2\left(\frac{\partial \Phi_{cp}}{\partial n_2}\right)_{n_1,T,P} \tag{2.9}$$

Combining Equations 2.7, 2.8, and 2.9 yields the expression for $\overline{C}_{p1}$

$$\overline{C}_{p1} = \overline{C}_{p1}^{\circ} - \frac{n_2^2}{n_1}\left(\frac{\partial \Phi_{cp}}{\partial n_2}\right)_{n_1,T,P} \tag{2.10}$$

For convenience in this work the concentrations of the solutions were expressed in molality, m, where m is the number of moles of solute per 1,000 gm of solvent, and heat capacities were expressed per unit mass, i.e., as specific heat capacities, S_p. Equation 2.8 for Φ_{cp} in terms of m and S_p becomes

$$\Phi_{cp} = \left(\frac{1{,}000}{m} + M_2 \right) S_p - \frac{1{,}000}{m} S_p^\circ \qquad (2.11)$$

where S_p is the specific heat capacity of the solution for which Φ_{cp} is being calculated, S_p° is the specific heat capacity of pure water, m is the molality of the solution, and M_2 is the molecular weight of the solute.

It is apparent that if S_p versus m data is taken over a range of concentrations for a particular rare earth salt, Φ_{cp} versus m data can be calculated for that salt utilizing Equation 2.11. To calculate $\overline{C}_{p1}$ and $\overline{C}_{p2}$ it is advantageous to have an analytical function expressing Φ_{cp} in terms of some composition variable. The variable chosen is $m^{1/2}$ as Φ_{cp} versus $m^{1/2}$ approximates a linear function. To convert Equations 2.9 and 2.10 for $\overline{C}_{p2}$ and $\overline{C}_{p1}$ to functions of $m^{1/2}$, the relations

$$n_2 = (m^{1/2})^2 \qquad (2.12)$$

and

$$n_1 = \frac{1{,}000}{M_1} \qquad (2.13)$$

are employed where M_1 is the molecular weight of water. Equations 2.9 and 2.10 then become respectively

$$\overline{C}_{p2} = \Phi_{cp} + \frac{1}{2} m^{1/2} \left(\frac{\partial \Phi_{cp}}{\partial m^{1/2}} \right)_{T,P} \tag{2.14}$$

$$\overline{C}_{p1} = \overline{C}_{p1}^{\circ} - \frac{M_1}{2,000} m^{3/2} \left(\frac{\partial \Phi_{cp}}{\partial m^{1/2}} \right)_{T,P} \tag{2.15}$$

$\overline{C}_{p1}$ and $\overline{C}_{p2}$, in addition to Φ_{cp}, can therefore be calculated from specific heat capacity versus molality data.

Although the absolute values of $\overline{C}_{p1}$ and $\overline{C}_{p2}$ are independent, the derivatives of $\overline{C}_{p1}$ and $\overline{C}_{p2}$ with respect to some composition variable are related. Taking the total differential of the function $C_p(n_1,n_2)$ in Equation 2.7 and subtracting Equation 2.7 yields

$$n_1 d\overline{C}_{p1} + n_2 d\overline{C}_{p2} = 0$$

It follows that

$$n_1 \frac{d\overline{C}_{p1}}{dn_2} = - n_2 \frac{d\overline{C}_{p2}}{dn_2}$$

or in terms of molality employing Equations 2.12 and 2.13

$$\frac{d\overline{C}_{p1}}{dm} = - \frac{mM_1}{1,000} \frac{d\overline{C}_{p2}}{dm} \tag{2.16}$$

Equation 2.16 relates the slopes of $\overline{C}_{p1}$ and $\overline{C}_{p2}$ versus m curves, and it is apparent that a minimum in the $\overline{C}_{p2}$ versus m curve will correspond to a maximum in the $\overline{C}_{p2}$ versus m curve and vice versa.

C. Theory of Heat Capacity for Aqueous Solutions of Electrolytes

The theory of Debye and Hückel predicts that in very dilute solutions the apparent molal heat capacity, Φ_{cp}, should be a linear function of the square root of concentration with a limiting slope of 89.9 for three to one charge type electrolytes (5). Spedding and Miller (22) found for dilute solutions of $NdCl_3$ and $CeCl_3$ that within experimental error Φ_{cp} was a linear function of $m^{1/2}$ with limiting slopes in good agreement with theory. However, the data in this work taken from 0.1 molal to saturation are beyond the concentration range where the simplifying assumptions made by Debye and Hückel are sound. Hence, these data cannot be used to test the validity of the Debye-Hückel theory.

The heat capacity of aqueous solutions of electrolytes approach that of pure water as the solutions become very dilute. Since the apparent molal heat capacity, Φ_{cp}, is a function of the difference between the heat capacity of the solution and that of pure water, any uncertainty in the measured heat capacity of a dilute solution causes a large

uncertainty in its Φ_{cp}. For example, an error of one part per 10,000 in the measured heat capacity of a 0.01 molal rare earth salt solution results in an error in Φ_{cp} of about 10 cal/deg mole. Since the heat capacities of solutions in this work were only measured to within five parts in 10,000, it was not of value to extend measurements down to the concentration range where the Debye-Huckel theory is effective.

At the present time there are no adequate quantitative theories for concentrated aqueous solutions of electrolytes. Therefore, the heat capacity data from this work cannot be compared with any theoretical values.

III. EXPERIMENTAL

A. Preparation and Analysis of Solutions

The specific heat capacities of the aqueous rare earth nitrate and perchlorate solutions were measured as a function of concentration from about 0.1 molal to saturation. From its specific heat capacity, Φ_{cp} was calculated for each of these solutions. Because Φ_{cp} versus $m^{1/2}$ approximates a linear function, the polynomial used to express Φ_{cp} as a function of concentration was expanded in orders of $m^{1/2}$. Therefore, an even distribution of data points across the concentration range was obtained by preparing solutions with increments of 0.1 in $m^{1/2}$. Usually this meant that 20 solutions were prepared.

In order to prepare these solutions, a large amount (~2,000 ml) of solution, henceforth called the stock solution, whose concentration approached saturation was first made. The 19 or so less concentrated solutions were then conveniently prepared from weighed portions of water and stock solution. The concentration of the rare earth salt in these solutions was calculated from the weights of water and stock solution which were known to ±0.001%, and from the concentration of the stock solution which was known to ±0.1%. Therefore, the accuracy of the calculated concentrations was almost entirely dependent on the uncertainty in the stock solution concentration. Because the less concentrated solutions were prepared

from the stock solution, this uncertainty was prorated resulting in a series of solutions whose relative concentrations were accurately known.

The stock solution was made by dissolving highly pure rare earth oxide in the C. P. grade acid corresponding to the salt that was desired. In order to remove colloidial species formed by the hydrolysis of the +3 rare earth ions and to assure a three to one ratio of anions to cations, the equivalence pH was determined. The equivalence pH is dependent on the degree of hydrolysis, of the type represented by Equation 3.1, that occurs.

$$RE^{+3} + H_2O = REOH^{+2} + H^{+} \qquad (3.1)$$

An initial titration was made to determine whether or not the pH of the solution was sufficiently greater than the equivalence pH to permit a complete titration curve to be obtained. If not excess oxide was added. The solution was filtered through a sintered glass filter to remove any oxide that did not dissolve. Another sample of the stock solution was titrated, and the equivalence pH was determined from the recorded pH versus titrant volume curves.

Using the correct acid, the stock solution was adjusted to the equivalence pH and then heated for a period of time not less than 12 hours to permit any colloidal species present to react with the acid. After cooling, the solution was

readjusted to the equivalence pH and again heated. This procedure was repeated until further heating and subsequent cooling did not affect the pH of the solution.

The stock solution was placed in a well-stoppered flask to prevent changes in concentration due to the exchange of water with the atmosphere. Depending on the humidity and the activity of water in the solution, the solution could either lose or gain water if left open to the air. The activity of water in some of the concentrated solutions was quite low, e.g., the activity of water in a 4.6 molal $Lu(ClO_4)_3$ solution was less than 0.15.[1]

The stock solution was then analyzed for rare earth salt concentration by at least two of the three methods outlined below. To obtain the constant weights of crucibles used in the two gravimetric methods, crucibles were repeatedly heated in a muffle furnace, cooled, and weighed. The crucibles were heated to 550°C for the sulfate method and to 900°C for the oxide method. The same procedure was used whether the crucibles were empty or contained precipitate.

1. Sulfate method. Samples of rare earth salt solutions were weighed into empty crucibles which were at constant weight. In the case of the nitrate solutions, hydrochloric acid was added and the solutions were gently heated on a hot plate to

---

[1]Spedding, F. H. and H. O. Weber, Ames, Iowa, Private communication, 1971.

decompose the nitrate anion and convert the rare earth nitrate to rare earth chloride. This was done to avoid coprecipitation of the nitrate with the sulfate. Enough one molar sulfuric acid was added to slightly exceed the stoichiometric requirements for forming the rare earth sulfate, then the solution was heated on a hot plate to drive off hydrochloric acid and sulfur trioxide formed by the decomposition of the excess sulfuric acid. The crucibles plus the resultant rare earth sulfate were then heated to constant weights.

In the case of the perchlorate solutions, enough one molar sulfuric acid was added to slightly exceed the stoichiometric requirements for forming the rare earth sulfate. The solution was heated on a hot plate to drive off the perchlorate ion as perchloric acid and sulfur trioxide formed by the decomposition of the excess sulfuric acid. Since it was possible a small number of perchlorate ions remained after this heating, rare earth perchlorate may have coprecipitated with the rare earth sulfate. The precipitate was heated at 550°C in a muffle furnace, cooled, and weighed. To obtain pure rare earth sulfate, a small amount of one molar sulfuric acid was added, and the heating and weighing steps repeated. This procedure gave the remaining perchlorate ion, if it was still intact, another chance to boil away as perchloric acid; or if the perchlorate ion had decomposed, the sulfuric acid converted the resultant rare earth oxide to the sulfate. When

repetition of this procedure did not cause a significant change in the weight of the precipitate, the crucibles plus the rare earth sulfate were repeatedly heated and cooled to obtain constant weights. The weight of anhydrous $RE_2(SO_4)_3$ was obtained from the difference in the constant weights of the crucibles empty and when containing the anhydrous $RE_2(SO_4)_3$. The rare earth salt concentration was calculated from the weight of the solution sample and from the weight of anhydrous $RE_2(SO_4)_3$.

2. Oxide method. Samples of rare earth salt solutions were weighed into empty crucibles which were at constant weight. The rare earth was precipitated with the addition of enough twice recrystallized oxalic acid to slightly exceed the stoichiometric requirements of the rare earth oxalate. The precipitate was dried on a hot plate, ignited to the oxide at 900°C in a muffle furnace, and repeatedly heated and cooled to obtain constant weight. The weight of anhydrous RE_2O_3 was obtained from the difference in the constant weights of the crucibles empty and when containing the anhydrous RE_2O_3. The rare earth salt concentration was calculated from the weight of the solution sample and from the weight of anhydrous RE_2O_3.

3. EDTA method (23). Samples of rare earth salt solutions were weighed into flasks, a few drops of pyridine were added as a buffer, and a few drops of xylenol orange were

added as indicator. Using a Sargent Model D recording titrator to monitor the pH and a dilute solution of NH_4OH to adjust the pH to five, the samples were titrated with weighted amounts of EDTA. The EDTA was standardized against $Gd(ClO_4)_3$ and $Lu(NO_3)_3$ solutions prepared by dissolving a weighed amount of the pure metal in the appropriate acid.

The concentration of a stock solution was taken as the average of the values determined by the two or more methods used. In all cases the value determined for the concentration (expressed in moles per gm) by one method agreed by 0.1% or better with the value(s) determined by the other method(s). For each method used at least duplicate and usually triplicate analyses were made with a precision of better than 0.1%.

From the analysis of the stock solution, calculations were made to determine the amounts of water and stock solution needed to prepare dilutions with 0.1 increments in their $m^{1/2}$ values. These dilutions were prepared by weight with these weights and all others throughout this work being corrected for the buoyancy of air. All water used for dilutions and elsewhere throughout this work was prepared by distillation from a solution of $KMnO_4$ and KOH. This water, henceforth called conductivity water, had a specific conductance of less than 1×10^{-6} mho per cm.

Saturated solutions were prepared by concentrating 300 to 500 ml portions of the stock solutions in a desiccator with $Mg(ClO_4)_2$ as the desiccant. When crystals formed, crystals and solution were placed in a flask attached to a rocker arm in a water bath at 25°C. After allowing two weeks or more for the solution to come to equilibrium with the crystals, samples of the clear saturated solution were decanted. The saturated solutions used in this work were analyzed for the concentration of rare earth salt by at least one of the three methods outlined previously. Triplicate analyses were made, and a precision of better than 0.1% obtained.

The rare earth oxides used in this work were analyzed for impurities by an emission spectrographic method. The results are shown in Table 1. Since C. P. grade acid was used and all glassware was cleaned with alcoholic KOH and soaked in conductivity water before being used, it was unlikely that any additional impurities would be found in solution. A check of the impurities in solution was made by a mass spectrographic method. The sample analyzed was Nd_2O_3 prepared from a $NdCl_3$ stock solution by the oxide method of analysis outlined previously. The $NdCl_3$ stock solution had been prepared and used by Jones (14,15). The results are shown in Table 2.

Table 1. Results of emission spectrographic analyses of rare earth oxides for impurities

Oxide	Analyses in percent[a]		
Pr_6O_{11}	Ca: ≷0.020	Y: <0.002	Nd: <0.100
	Fe: <0.003	La: <0.002	Sm: <0.007
	Si: <0.025	Ce: <0.050	
Sm_2O_3	Ca: <0.002	Y: <0.005	Eu: 0.010
	Fe: ≷0.004	Pr: 0.020	Gd: ≷0.030
	Si: 0.004	Nd: 0.020	
Tb_4O_7	Ca: 0.001	Y: ≷0.008	Dy: ≷0.010
	Fe: ≷0.002	Sm: ≷0.020	
	Si: ≷0.002	Gd: ≷0.020	
Dy_2O_3	Ca: <0.002	Y: ≷0.001	Ho: 0.010
	Fe: ≷0.007	Gd: 0.020	Er: <0.005
	Si: ≷0.010	Tb: 0.050	
Ho_2O_3	Ca: 0.005	Y: ≷0.001	Tm: <0.020
	Fe: ≷0.003	Dy: <0.015	
	Si: ≷0.003	Er: ≷0.050	
Er_2O_3	Ca: 0.002	Y: ≷0.001	Tm: <0.010
	Fe: 0.002	Dy: ≷0.010	Yb: <0.005
	Si: 0.006	Ho: <0.005	
Tm_2O_3	Ca: 0.003	Ho: ≷0.020	Lu: ≷0.030
	Si: <0.006	Er: ≷0.003	
	Y: ≷0.001	Yb: 0.008	
Yb_2O_3	Ca: 0.040	Er: ≷0.005	Th: ≷0.020
	Fe: 0.005	Tm: ≷0.005	
	Y: 0.005	Lu: ≷0.005	

[a]A less-than symbol, <, indicates the element was detected but is present in an amount less than the number reported which is the lower limit of the quantitative analytical method. A bar over the less-than symbol, ≷, indicates the element was not detected and the number reported is again the lower limit of the quantitative analytical method. Therefore, when either of these symbols is used, the actual amount of impurity present may be much less than the value reported.

Table 2. Results of mass spectrographic analysis of Nd_2O_3 for impurities

Element	ppm[a]	Element	ppm	Element	ppm
K:	5.	Ag:	<0.5	Tm:	≤1.
Ca:	350.	Cd:	<0.2	Yb:	≤4.
Sc:	1.	In:	<0.1	Lu:	≤0.5
Ti:	40.	Sn:	<0.3	W:	<5.
V:	2.	Sb:	<0.06	Re:	<2.
Cr:	10.	Te:	≤1.	Os:	<4.
Mn:	10.	Cs:	≤1.	Ir:	<1.
Fe:	30.	Ba:	0.9	Pt:	<1.
Co:	<0.3	La:	≤50.	Au:	<0.3
Ni:	14.	Ce:	2.	Hg:	<0.5
Cu:	20.	Pr:	<0.3	Tl:	<0.3
Zn:	2.	Sm:	20.	Pb:	<0.6
Y:	10.	Eu:	0.06	Bi:	<0.2
Zr:	<0.5	Gd:	≤20.	Th:	<0.3
Mo:	2.	Tb:	≤20.	U:	<0.3
Ru:	<1.	Dy:	≤5.		
Rh:	<0.5	Ho:	≤0.4		
Pd:	<2.	Er:	≤6.		

[a]Amounts of impurities reported in atomic ppm with Nd = 10^6 ppm as reference (≤ indicates less than or equal to).

B. Description of Calorimeter

Calorimeters are instruments used to measure the heat involved for a known change of state of a material. This change in state may mean a change in temperature, phase, chemical composition, pressure, volume, or any combination

of these. Different calorimeters are used depending on the requirements of the particular problem. Sources of information on modern calorimetry are provided by Osborne and Stein (24), Sturtevant (25), Rossini (26), Skinner (27), and Swietoslawski (28). Armstrong (29) provides a major survey of the historical evolution of the calorimeter and its influence on the development of chemistry.

The calorimeter used in this work to measure the specific heat capacities of solutions was an adiabatic single can solution calorimeter built by K. C. Jones (14,15) and used by J. P. Walters (16). The calorimeter was essentially adiabatic because the sample was separated from the surroundings by a near vacuum of the order of 10^{-5} torr, and the temperature of the surroundings was kept as close to that of the sample as possible. To insure chemical inertness all parts of the apparatus to come in contact with the sample were constructed of tantalum.

The temperature of the stirred sample was sensed by a thermistor and was continually registered on a strip-chart recorder as the imbalance of a Wheatstone bridge constructed with the thermistor in one arm and constant resistances in the other arms. The sample was heated electrically, and the quantity of heat added could be calculated knowing the resistance of the heater, the current flowing through it, and the length of time of current flow. The value obtained for the specific heat capacity as calculated from the quantity

of heat added and the resultant temperature rise was accurate to ±0.05%.

Schematic diagrams of the calorimeter and sample container are shown in Figures 1 and 2, respectively. Figure 3 is a schematic diagram of the electrical circuits. The figures will be referred to numerically and each labeled part of the figures alphabetically, e.g., Figure 1-X.

1. Sample container and stirrer

The sample was contained in a 110 ml can (Figure 1-L and 2-N) of welded 20 mil tantalum, 1-15/16 inches in diameter and 2-7/16 inches deep. Because a vacuum was created in the volume (Figure 1-M) surrounding the sample container, the sample container had to be airtight. Using Torr Seal low-pressure epoxy resin, an aluminum "O" ring seat (Figure 2-E) was attached to the can. With a rubber "O" ring greased with Apiezon N grease in this seat, the can was made to form an airtight seal with the lid by screwing the threaded ring (Figure 2-K) onto the threaded ring (Figure 2-J) that was attached to the lid with Torr Seal.

The lid of the sample container was attached by a threaded lug to a brass flange (Figure 2-D) which was silver soldered to the hanger tube (Figure 2-B). The hanger tube which provided support and housed the stirrer shaft was attached to the submarine lid. This tube was a 1/2 inch diameter, 1-3/4 inch long, 6 mil stainless steel tube. Six mil tubing was used

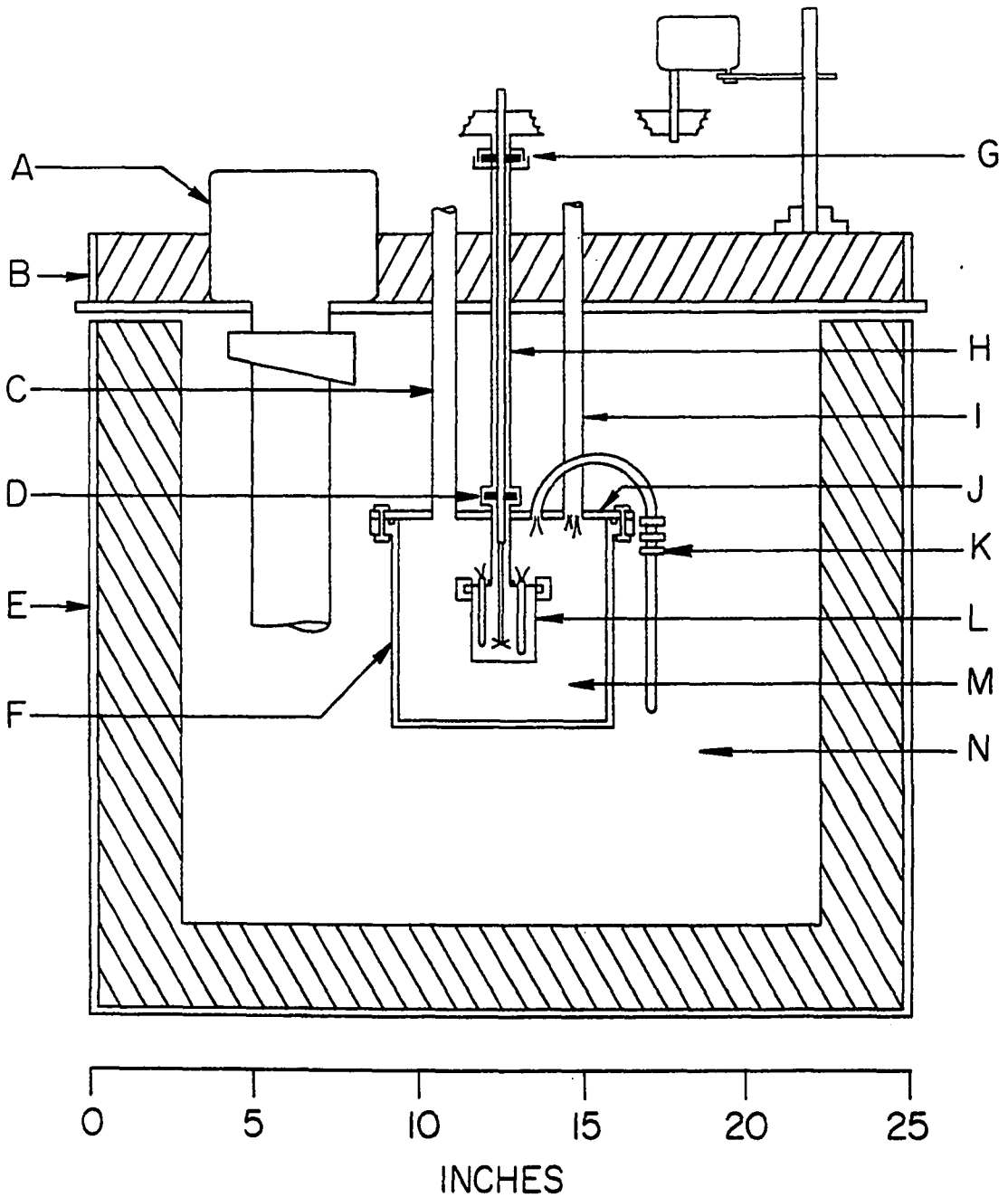

Figure 1. Assembled adiabatic solution calorimeter

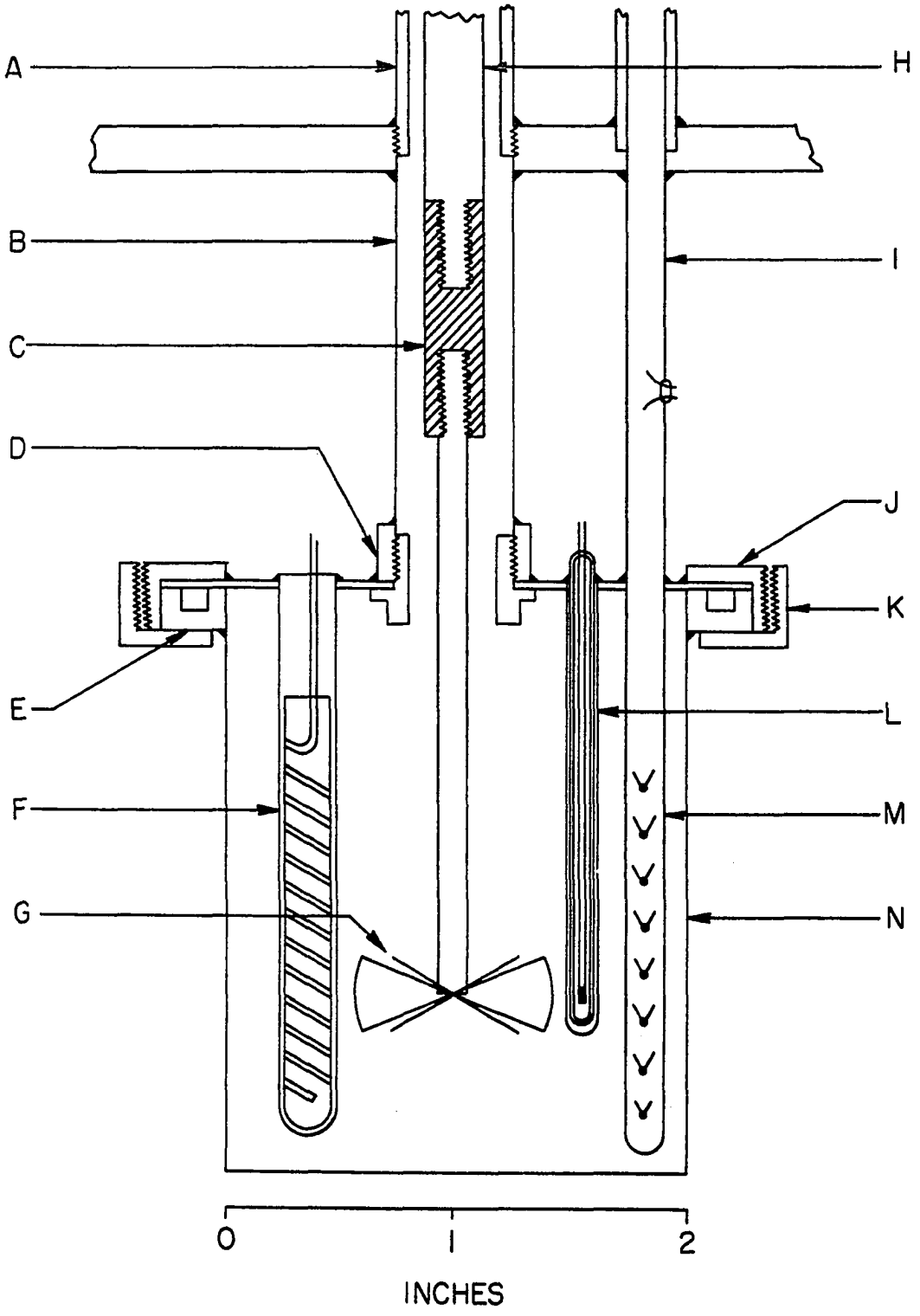

Figure 2. Sample container plus appendages

to minimize heat conduction between the sample and surroundings.

The sample was stirred to keep the temperature uniform by the 7/8 inch diameter four-bladed tantalum propellor (Figure 2-G). To reduce thermal conduction between the sample and the surroundings, the stirrer shaft included a lucite spacer (Figure 2-C). The stirrer shaft (Figure 2-H) was a 1/4 inch diameter stainless steel shaft held in place by two bearings (Figure 1-D and 1-G). At the top of this shaft around the upper bearing (Figure 1-G) was a vapor seal consisting of an inverted brass cup immersed in Cenco Hyvac oil. A 300 rpm type KYC-23RB Bodine motor in combination with two three-gang pulleys provided nine constant stirring speeds from 105 to 325 rpm. A maximum of stirring with a minimum of heating was desired. To minimize the heat of stirring and the subsequent correction made for it, slower stirring speeds were necessary to stir the more viscous concentrated solutions.

2. Submarine and vacuum system

The submarine jacket (Figure 1-F) was a cylindrical monel vessel 6-1/2 inches in diameter and 6-1/2 inches high. The cylindrical wall was 1/6 inch thick and the base 1/8 inch thick. Silver soldered to the top of the submarine jacket was a brass collar with an "O" ring seat. This collar was tapped to hold eight machine screws which were used to attach the submarine jacket to the submarine lid. With an "O" ring greased with Apiezon N grease in the "O" ring seat,

the submarine jacket was made to form an airtight seal with the submarine lid. The submarine lid was a monel disk 7-1/2 inches in diameter and 1/4 inch thick. To provide support, the lid was silver soldered to three 1/2 inch diameter brass tubes. Two of these tubes (Figure 1-I, one not shown) also provided passages for wiring, and the third (Figure 1-H, Figure 2-A) also enclosed the stirrer shaft.

In order to isolate the sample from the surroundings by as much as possible and thus minimize heat flow, the submarine jacket could be evacuated. The air was pumped from the submarine jacket through the one inch diameter copper tube (Figure 1-C) by means of a model 1400 Duo-Seal mechanical fore pump and a mercury diffusion pump. To prevent the diffusion of mercury to other parts of the system, liquid nitrogen cold traps were placed in the vacuum line before and after the mercury diffusion pump. The vacuum line was an 8/10 inch Pyrex tube and contained a 15 mm Pyrex vacuum stopcock. This line was connected to the copper tube by means of a glass to metal seal. The pressure was measured by a type BA100P GCA ionization gauge, powered by a type 710 NRC ionization controller. When the vacuum system was in use, the pressure in the system was usually less than 1×10^{-5} torr and always less than 2×10^{-5} torr.

3. Water bath and temperature control

The temperature of the room in which the calorimeter was housed was maintained at 24.0 ± 0.5°C. In order to provide an environment for the submarine and calorimeter assembly with less temperature fluctuation than ±0.5°C, the calorimeter included a 22 gallon water bath (Figure 1-N) that could be raised by means of a hydraulic jack to surround the submarine jacket. This bath was stirred, with a minimum of heating, by a 100 gallon per minute type NSI-53 Bodine stirrer (Figure 1-A) suspended from the bath lid (Figure 1-B). The bath lid was held in a fixed position 55 inches from the floor by an angle iron frame. The lid, floor, and wall (Figure 1-E) of the bath were all double walled, and the three inch space between walls was filled with exploded mica insulation.

The proportional control system responsible for maintaining the temperature of the bath as close to that of the sample as possible consisted of four major components:

1. A differential temperature sensor.
2. A detector which detected and amplified the output of the sensor.
3. A control unit which automatically produced a signal proportional to the amplified output of the sensor.
4. A power source that translated the signal from the control unit into heat input to the water bath.

The differential temperature ($\theta_b - \theta_s$) between the water bath and the sample was sensed by an eight junction copper-constantan thermopile. The eight junctions immersed in the water bath were spaced at 3/4 inch intervals in a copper tube (Figure 1-K). The eight junctions immersed in the sample were spaced at 1/4 inch intervals in a tantalum well (Figure 2-M). In the evacuated space between the submarine lid and the sample lid, the thermopile wires were housed in a 1/8 inch diameter 6 mil stainless steel tube sealed at both lids with Torr Seal (Figure 2-I). Leads from the thermopile exited the tube through a small hole made vacuum tight with Torr Seal.

The signal from the thermopile was detected and amplified by a Leeds & Northrup type 9834 electronic D-C null detector. This signal was continuously registered on a strip-chart recorder. The control unit was a Leeds & Northrup Series 60 current adjusting type. The power source was a Leeds & Northrup type 10915-25 power package.

The power source as directed by the control unit provided heat input to the bath by means of a 29 ohm calrod heater. The bath was constantly cooled by the passage of cold water through a two turn copper cooling coil. This control system maintained the temperature of the water bath within ±0.0005°C of that of the sample.

During the nine minute period while the sample was being heated and its temperature raised, the temperature of the bath was simultaneously raised using an auxiliary heater.

This heater was a 19 ohm calrod heater, and the power supplied it was regulated manually by a powerstat. Under proper regulation the bath temperature was maintained within ±0.002°C of that of the sample during the heating period.

For the small temperature differences involved, Newton's Law of Cooling can be assumed to be valid. Therefore,

$$Q = A \int (\Theta_b - \Theta_s) \, dt \qquad (3.2)$$

where Q equals the net heat that flowed from the water bath to the sample, A is the heat leak constant, t is time and Θ_b and Θ_s are the temperature of the water bath and of sample, respectively. The heat leak constant, A, had been determined previously to be 0.3 cal deg C^{-1} min^{-1} (16). The fluctuation of the water bath temperature around the temperature of the sample was such that the negative and positive areas of the integral in Equation 3.2 were nearly equal. Q was therefore very small, and a correction for heat leak was not made.

4. Measurement of temperature

The sensor used to measure the temperature of the sample was a Fenwall #6462 glass probe type thermistor which was housed in a tantalum well (Figure 2-L). At 25°C the thermistor had a resistance of 110,000 ohms with a temperature coefficient of resistance of -5,000 ohms per deg C. The thermometer circuit as shown in Figure 3 contained a Wheatstone bridge with the thermistor and a variable resistor in one arm and

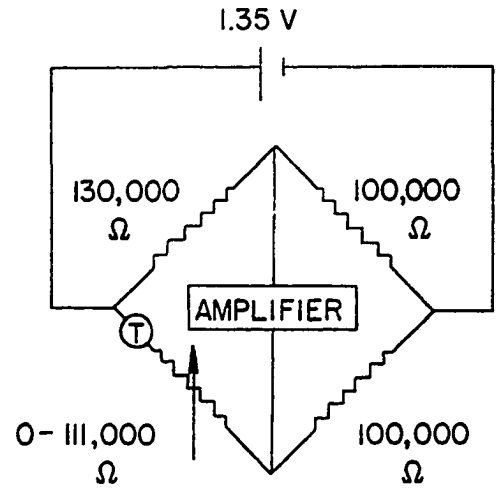

THERMOMETER CIRCUIT

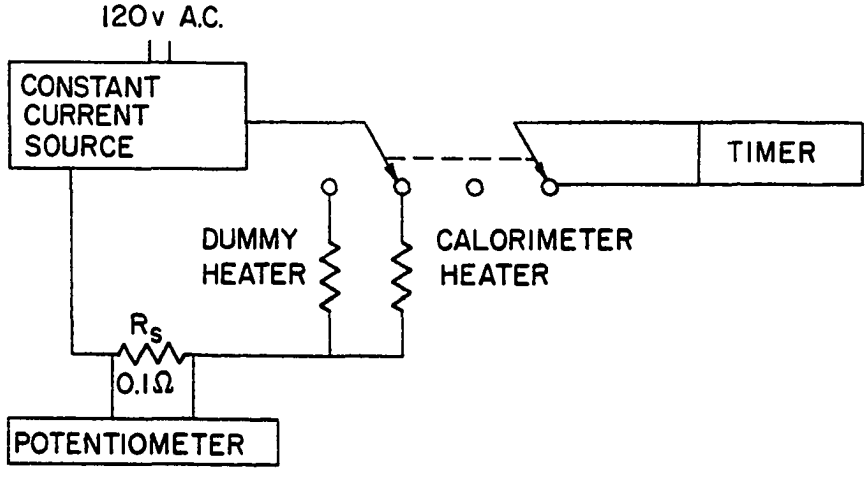

HEATER CIRCUIT

Figure 3. Calorimeter thermometer and heater circuits

constant resistors in the other three arms. The constant resistors were type 1441 General Radio Company resistors stable to ±0.003% per year. The variable resistor was a type 1432 General Radio Company resistor with a range from 0 to 111,111 ohms in 0.1 ohm steps.

To maintain the stability of the thermistor, power was continuously supplied to the Wheatstone bridge containing the thermistor by two 1.35 volt mercury cells in parallel. Care was taken not to shock the thermistor either thermally or mechanically. A periodic check was made to insure that the thermistor's behavior was invariant.

The temperature, as measured by the resistance of the thermistor, was determined from the resistance setting of the variable resistor and the imbalance of the Wheatstone bridge. The signal due to the imbalance of the bridge was amplified by a Kintel model 11BF d.c. chopper amplifier and registered on a 10 millivolt strip-chart recorder. Under amplification of 280 times, a millimeter displacement on the chart corresponded to a 0.1 ohm change in the resistance of the thermistor or to a change of 2×10^{-5} deg C in the temperature of the sample.

In order to determine how the resistance of the thermistor varied with temperature, a calibration was made by immersing both the thermistor and a platinum resistance thermometer, previously calibrated by the National Bureau of

Standards, in a 400 ml vessel filled with water. To maintain uniform temperature, the water was well stirred. To prevent cooling due to the evaporation of water, the water was covered with a layer of mineral oil. The calibration was made from 23.3°C to 26.7°C in 0.1°C intervals. At each point the temperature was calculated from the resistance of the platinum resistance thermometer as measured by a calibrated Leeds & Northrup G-2 Mueller bridge.

To simplify calculations, this temperature was recorded versus the resistance reading of the variable resistor rather than the resistance of the thermistor. This is legitimate because with the bridge balanced

$$R_t = K - R_v$$

and

$$dR_t/d\theta = -dR_v/d\theta$$

where R_t equals the thermistor's resistance at the given temperature, K is some unknown constant, R_v is the variable resistance reading at the same temperature, and θ equals temperature.

The θ versus R_v data was fit, using the method of least squares, to the fourth order equation

$$\theta = A + BR_v + CR_v^2 + DR_v^3 + ER_v^4 \qquad (3.3)$$

with θ given in degrees C; R_v in ohms. The constants A, B,

C, D, and E were determined with the aid of the computer. The average deviation between Θ experimental and Θ calculated from the fit was about 5×10^{-5}°C.

This calibration was repeated every six months in order to insure that the constants in Equation 3.3 were still valid. It was necessary in determining the specific heat capacity of a solution to measure temperature differences as accurately as possible. It was not necessary to know the absolute temperature to better than 0.1°C since the specific heat capacity of a solution at 25°C was taken as the average of three measurements over the temperature range 24.4°C to 25.6°C. Therefore, the constant, A, in Equation 3.3 is not important. Typically successive calibrations resulted in changes of the absolute temperature, as calculated from Equation 3.3, of 0.002°C, whereas temperature differences as calculated from Equation 3.3 changed by only 0.02% in the temperature range 24.4°C to 25.6°C.

5. Measurement of heat

The heater used to raise the temperature of the sample consisted of 63 inches of 38 B and S gauge double silk covered manganin wire with two 30 B and S gauge copper leads. The manganin wire was noninductively wound on a thin-walled copper tube which was fitted in a tantalum well (Figure 2-F). The heater's resistance was 95 ohms and changed by less than 0.01% in a two year period.

The heater circuit is shown in Figure 3. Sixty milliamperes current was supplied to the heater by the constant current source built by the Ames Laboratory's electronics shop. This source was constant to ±0.01 milliamperes during the nine minute heating periods. To maintain the stability of the constant current source, the current was shunted through a 95 ohm dummy heater when the sample was not being heated.

The current flowing through the heater was calculated from the potential drop across a 0.1 ohm standard resistor in series with the heater. The standard resistor was calibrated by the National Bureau of Standards and kept thermostated at 25°C in an oil bath. The potential drop was measured by a Leeds & Northrup K-3 potentiometer. A Leeds & Northrup constant voltage supply #099034 provided the potentiometer with a constant potential, and the standard cell used for calibration of the potentiometer was calibrated by the Ames Laboratory's electronics shop.

When the heater was turned on, the timer was simultaneously activated. The electronic timer used a five megacycle quartz crystal frequency standard whose output was divided down to 1,000 cycles per second by a series of flip-flop frequency dividers. By counting cycles the timer was capable of measuring time intervals to 0.001 second.

C. Procedure Used

1. Operation of calorimeter

When a heat capacity measurement was made, the total heat capacity of the sample plus the sample container and appendages was determined. To determine the heat capacity of the sample alone, the heat capacity of the sample container and appendages, henceforth denoted W, had to be subtracted from the total heat capacity.

$$C_{p\ sample} = C_{p\ total} - W \qquad (3.4)$$

In order to determine a value for W, $C_{p\ total}$ was determined for a sample of known heat capacity, and W was calculated from the relationship in Equation 3.4. Conductance water, saturated with air, was used as the sample in this determination. Therefore, $C_{p\ sample}$ was equal to the specific heat of air-saturated water, assumed to be 0.9989 cal/deg C gm (30), times the sample mass. It was found (14) that W was a function of the sample volume because of the indefinable nature of the boundary between the sample container plus appendages and the surrounding submarine jacket and water bath. Rather than determine this function, all samples were weighed into the sample container such that they had essentially the same volume of 104.82 ±0.01 ml.

In determining the total heat capacity, $C_{p\ total}$, both the sample and the calorimeter water bath were cooled to a temperature less than 24°C. The sample was weighed into the sample container to 0.1 mg. After attaching the sample container and submarine jacket to their respective lids, the vacuum pumps were started, and the water bath raised to surround the submarine jacket. By adding heat to the sample or the water bath, depending on which one was cooler, the temperatures of the sample and the water bath were equalized and the control system was activated. Following a two hour waiting period, the pressure in the submarine jacket was less than 2×10^{-5} torr and the temperature drift of the sample and its container plus appendages had become linear with time. Because the sample and its container plus appendages were separated from the surrounding by essentially adiabatic conditions, the slope of the temperature drift with time curve should have been nearly zero. However, the samples were well stirred, and the heat due to stirring caused the temperature versus time curve to have a positive slope of approximately 4×10^{-5}°C per minute.

To ensure that all parts of the calorimeter were functioning properly and to raise the temperature of the sample and the water bath to the desired temperature of 24.4°C, a dummy heat capacity run was made. The temperature 24.4°C was chosen as the initial temperature because this allowed

three heat capacity determinations with 0.4°C intervals to be made in the range of 24.4°C to 25.6°C with the average temperature of these determinations being 25.0°C.

Following the dummy heat capacity run, at least 30 minutes of linear behavior for the temperature versus time curve were registered before the d.c. power source was switched from the dummy heater circuit to the sample heater circuit, and the auxiliary water bath heater was switched on. The d.c. power source had been previously set to cause the sample temperature to rise 0.4°C in a nine minute heating period. At the end of this heating period, it took from 15 to 20 minutes for the sample temperature to become uniform and the temperature versus time curve to become linear again. After at least 30 minutes of linear behavior, this procedure was repeated two more times spanning the temperature interval 24.4°C to 25.6°C and resulting in three heat capacity determinations.

The quantity of electrical heat added, Q, was calculated from the equation

$$Q = R_h E_s^2 t \,/\, 4.18400\, R_s^2 \qquad (3.5)$$

where R_h is the resistance of the sample heater in ohms, E_s is the potential drop across the standard resistor in volts, t is the time in seconds, R_s is the resistance of the standard resistor in ohms, and 4.18400 is a conversion factor (one

calorie = 4.18400 absolute joules). The quantity E_s was an average of 18 values taken at 30 second intervals during a nine minute heating period. It was permissible to average E_s values rather than E_s^2 values as employed in Equation 3.5 because the average deviation of E_s values from the mean value was always less than 0.01%. The quantity of heat added was determined to better than 0.01%.

Straight lines were drawn through the temperature versus time curves to determine the slope of these curves before and after a heat. The values for the fore and after slopes were slightly different because the viscosity of the sample changed with temperature. The initial temperature, θ_i, was taken as the temperature just before the heating period began, and θ_f was taken as the temperature 24 minutes later. Twenty-four minutes was chosen as a time interval because usually in this amount of time the temperature of the sample was uniform and the temperature versus time curve was linear again. If the temperature versus time curve was not yet linear after 24 minutes, the temperature was measured from a straight line extrapolation from the time that the curve did become linear.

The temperature difference as calculated from $\theta_f - \theta_i$ included a temperature change due to the heat of stirring for the 24 minute interval between the time when θ_i was taken and the time when θ_f was taken. A correction, θ_c, for the temperature increase due to stirring was made using an average

of the fore and after slopes such that

$$\Delta\theta = \theta_f - \theta_i - \theta_c$$

and

$$\theta_c = 24 \frac{S_f + S_a}{2}$$

where $\Delta\theta$ is the temperature rise due to the addition of electrical heat only and S_f and S_a are the fore and after slopes, respectively, in deg C per min. This correction was usually less than 0.001°C.

Because the vapor pressure of water increases with temperature, some of the heat added to the sample in going from θ_i to θ_f was absorbed to keep the air over the sample saturated with water vapor. The heat capacity of the sample and its container plus appendages as calculated from $Q/\Delta\theta$ was corrected for this vaporization by the method of Hoge (31). The correction was always less than 0.02% of the heat capacity of the sample.

The heat capacity of the sample container plus appendages, W, was taken as the average of values from several determinations using water as the sample. A typical value determined for W was 16.95 ±.02 cal/deg C.

2. Specific heat of solutions and accuracy of method

The same procedure that was used in the determination of $C_{p\ total}$ with water as the sample was used with a solution

as the sample. However, slower stirring speeds were used to minimize the heat of stirring in the more viscous solutions. The heat capacity of the solution was calculated employing Equation 3.4. The heat capacity of 104.82 ml of solution was in the vicinity of 100 cal/deg C, so an average deviation of ±0.02 cal/deg C in the determination of W would result in an error of only 0.02% in the heat capacity of a solution.

The three values obtained for the heat capacity of the solution were divided by the sample mass to give three values for the specific heat capacity. The average of these three values was taken as the specific heat capacity, and Φ_{cp} was calculated from this average and the molality of the solution.

To check the accuracy of the calorimeter and of the values determined for W, the specific heat capacities of several NaCl solutions were measured during the course of this work and compared to those obtained by Randall and Rossini (32), hereafter referred to as R & R. In order to make the comparison, R & R's data were recalculated using defined calories and atomic weights based on carbon-12, and using the computer a fourth order least squares fit of specific heat capacity versus molality was obtained for their data.

The results are listed in Table 3. As is apparent from the Δ values, which are differences between the specific heat capacities listed in column three and those of R & R, the values obtained in this work were all slightly lower than

those obtained from R & R's data. Likewise, the results obtained by Jones (15) and Walters (16) using the same calorimeter as was used in this laboratory were consistent with values for S_p obtained in this work and were lower than those of R & R. It is possible that the fact Δ was always negative has no meaning since the differences were within the limits of the combined experimental errors of the two methods used to obtain S_p values. However, if the differences are real, the fact that Δ was always negative would imply a systematic error was made either in this laboratory or in R & R's work.

Also listed in Table 3 are values for the specific heat capacities of three NaCl solutions as measured by Russian scientists (33). From a comparison of their values with those of R & R, it appears that the Russian values are more in line with those obtained in this work, and that a systematic error, if one exists, was made by R & R. From the agreement and precision of the data as listed in Table 3, an accuracy of at least $\pm 0.05\%$ in the determination of specific heat capacities of solutions was assumed.

Table 3. Specific heat capacity of aqueous NaCl solutions at 25°C

m	number of determinations	S_p	S_p[a] R & R	Δ
		cal/deg gm		
0.50022	9	0.9636±0.0002[b]	0.9639	-0.0003
0.50646	12	0.9631±0.0001	0.9635	-0.0004
1.0054	21	0.9340±0.0001	0.9343	-0.0003
1.3200	9	0.9177±0.0001	0.9182	-0.0005
1.3509	9	0.9163±0.0003	0.9167	-0.0004
2.1221	24	0.8826±0.0001	0.8832	-0.0006
2.5096	9	0.8680±0.0004	0.8689[c]	-0.0009
0.9956		0.9345[d]	0.9349	-0.0004
1.9959		0.8875	0.8882	-0.0007
2.4797		0.8690	0.8699[c]	-0.0009

[a]Values of S_p obtained from the fourth order least squares fit of R & R's data.

[b]Average deviation from the mean for this work.

[c]Value of S_p obtained by extrapolation of the fourth order equation beyond R & R's last data point at 2.2966 m.

[d]S_p data from Russian work (33).

IV. CALCULATIONS AND RESULTS

A. Treatment of Data

The specific heat capacity for each solution was taken as the average of values from three determinations. The apparent molal heat capacity, Φ_{cp}, was then calculated for each solution from its specific heat capacity and molality using Equation 2.11

$$\Phi_{cp} = \left(\frac{1{,}000}{m} + M_2 \right) S_p - \frac{1{,}000}{m} S^{\circ}_p \qquad (2.11)$$

An empirical polynomial equation of the type

$$\Phi_{cp} = A + Bm^{1/2} + Cm + Dm^{3/2} + \cdots \qquad (4.1)$$

was obtained for each salt. These equations which express Φ_{cp} as a function of $m^{1/2}$ were obtained from a least squares fit of Φ_{cp} versus $m^{1/2}$ data with the aid of the computer. Each Φ_{cp} point was weighted proportionately to the square of the inverse of the probable error in Φ_{cp} (the calculation of probable errors is discussed later in this chapter). A third order equation (four coefficients) was sufficient to express Φ_{cp} as a function of $m^{1/2}$ for the rare earth perchlorates. A fourth order equation was sufficient for the rare earth nitrates with the exceptions of $Tm(NO_3)_3$

and $Yb(NO_3)_3$ which required sixth order equations to adequately express Φ_{cp} as a function of $m^{1/2}$.

Substituting the expression for Φ_{cp} from Equation 4.1 into equation 2.15 and 2.14 results in the following equations for the partial molal heat capacity of the solvent, $\overline{C}_{p1}$, and the partial molal heat capacity of the solute, $\overline{C}_{p2}$, respectively.

$$\overline{C}_{p1} = \overline{C}_{p1}^{\circ} - \frac{M_1}{2{,}000} (Bm^{3/2} + 2Cm^2 + 3Dm^{5/2} + \cdots\cdot) \qquad (4.2)$$

$$\overline{C}_{p2} = A + 3/2\ Bm^{1/2} + 2Cm + 5/2\ Dm^{3/2} + \cdots\cdot \qquad (4.3)$$

$\overline{C}_{p1}$ and $\overline{C}_{p2}$ were calculated from Equations 4.2 and 4.3 for each salt using the coefficients from the least squares fits. The value of $\overline{C}_{p1}^{\circ}$ was taken as 17.996 cal/deg mole (30), and molecular weights throughout this work were calculated from the International Atomic Weights for 1969 (based on carbon-12).

B. Results

The coefficients of the empirical equations expressing Φ_{cp}, $\overline{C}_{p1}$ and $\overline{C}_{p2}$ as a function of $m^{1/2}$ for each salt are listed in Table 4. The molality (m), square root of molality ($m^{1/2}$), specific heat (S_p), experimental apparent molal heat capacity (Φ_{cp}), apparent molal heat capacity calculated from the least squares fit (Φ_{cp} L.S.), and the difference between the two Φ_{cp} values (Δ) are listed in Tables 5 through 19 for each solution of each salt run. Values of Φ_{cp}, $\overline{C}_{p1}$ and $\overline{C}_{p2}$ calculated at rounded values of m from Equations 4.1, 4.2, and 4.3 respectively for the rare earth nitrates and perchlorates are listed in Tables 20 through 25. Included in Tables 4 and 20 through 25 are the results obtained by Walters (16). In Figures 4 through 7 the heat capacity properties of the nitrate, perchlorate, and chloride salts of Pr, Sm, Dy, and Yb are plotted versus molality. The data for the plots of the chloride salts were obtained from the work of Jones (14,15) and Walters (16). The four rare earths; Pr, Sm, Dy, and Yb were chosen as representative elements across the rare earth series.

C. Error Analysis

Φ_{cp} as calculated from Equation 2.11 is a function of the two variables m and S_p. These two variables were measured independently, and therefore errors in one variable are independent of errors in the other. The principle of

Table 4. Coefficients for calculating Φ_{cp}, $\overline{C}_{p1}$ and $\overline{C}_{p2}$ from Equations 4.1, 4.2 and 4.3

Salt	A	B	C	D	E
$La(ClO_4)_3$[a]	-50.180	85.2638	-34.6529	7.43040	
$Pr(ClO_4)_3$	-52.039	86.2580	-34.9307	7.86312	
$Nd(ClO_4)_3$[a]	-54.156	94.3404	-40.8012	9.05382	
$Sm(ClO_4)_3$	-47.430	82.7575	-34.1919	8.15268	
$Gd(ClO_4)_3$[a]	-42.218	83.2694	-37.2393	8.72292	
$Tb(ClO_4)_3$	-40.272	84.4843	-37.9785	8.71321	
$Dy(ClO_4)_3$	-37.900	79.1418	-32.2813	7.00274	
$Ho(ClO_4)_3$	-34.614	72.8674	-26.8668	5.62996	
$Er(ClO_4)_3$	-38.706	80.2874	-32.0443	6.88503	
$Tm(ClO_4)_3$	-33.514	69.5713	-24.2234	5.23060	
$Yb(ClO_4)_3$	-40.617	80.3706	-29.7973	6.08571	
$Lu(ClO_4)_3$[a]	-40.363	81.3709	-30.9580	6.19899	
$La(NO_3)_3$[a]	-68.391	60.3704	33.2025	-25.32398	4.24424
$Pr(NO_3)_3$	-71.514	77.6857	6.8721	-10.55265	1.56570
$Nd(NO_3)_3$[a]	-65.829	69.7385	7.0259	-7.41643	0.57724
$Sm(NO_3)_3$	-59.886	57.5473	14.2082	-9.56360	0.92723
$Gd(NO_3)_3$[a]	-58.426	58.6040	7.1748	-4.03456	-0.34127
$Tb(NO_3)_3$	-63.744	65.6585	7.7528	-7.52887	0.73957
$Dy(NO_3)_3$	-56.685	38.8256	42.1320	-24.35666	3.48513
$Ho(NO_3)_3$	-56.711	31.4035	55.3502	-31.47169	4.71652
$Er(NO_3)_3$[a]	-44.450	-15.8027	116.7107	-61.77694	9.74630
$Tm(NO_3)_3$	-82.644	179.2362	-266.3302	314.46424	-184.29746
			(F = 50.517035, G = -5.271952)		
$Yb(NO_3)_3$	-83.734	196.6221	-318.4657	372.34879	-212.20693
			(F = 56.315454, G = -5.664555)		
$Lu(NO_3)_3$[a]	-108.276	324.5424	-576.9362	622.65435	-335.50379
			(F = 86.129475, G = -8.477328)		

[a]Results obtained by Walters (16).

Table 5. Specific heat capacity and apparent molal heat capacity of aqueous $Pr(NO_3)_3$ solutions at 25°C

m	$m^{1/2}$	S_p cal/deg gm	Φ_{cp}	Φ_{cp} L.S.[a] cal/deg mole	Δ
0.094464	0.30735	0.9445	-48.9	-47.3	1.6
0.16761	0.40940	0.9408	-39.0	-39.2	-0.2
0.25900	0.50892	0.9136	-30.5	-31.5	-1.0
0.37494	0.61232	0.8818	-24.0	-23.6	0.4
0.51372	0.71674	0.8484	-15.6	-15.8	-0.2
0.67033	0.81874	0.8174	-8.4	-8.4	0.0
0.84770	0.92071	0.7812	-1.4	-1.3	0.1
1.0470	1.0232	0.7484	5.5	5.6	0.1
1.2769	1.1300	0.7158	12.3	12.4	0.1
1.5195	1.2327	0.6863	18.6	18.5	-0.1
1.7882	1.3372	0.6580	24.5	24.4	-0.1
2.0826	1.4431	0.6316	30.1	30.0	-0.1
2.3973	1.5483	0.6071	35.0	35.1	0.1
2.7450	1.6568	0.5841	39.8	39.9	0.1
3.1058	1.7623	0.5636	44.1	44.1	0.0
3.4996	1.8707	0.5441	47.9	47.9	0.0
3.9175	1.9793	0.5261	51.3	51.4	0.1
4.3591	2.0878	0.5099	54.5	54.4	-0.1
4.8340[b]	2.1986	0.4938	56.9	56.9	0.0
5.0180[b]	2.2401	0.4880	57.8	57.8	0.0
				Average	±0.2

[a]Calculated from Equation 4.1 using coefficients given in Table 4.

[b]Saturated solution.

Table 6. Specific heat capacity and apparent molal heat capacity of aqueous $Sm(NO_3)_3$ solutions at 25°C

m	$m^{1/2}$	S_p cal/deg gm	Φ_{cp}	Φ_{cp}[a] L.S. cal/deg mole	Δ
0.090965	0.30160	0.9652	-46.0	-41.5	4.5
0.16061	0.40076	0.9424	-34.9	-35.1	-0.2
0.24919	0.49919	0.9153	-27.5	-28.7	-1.2
0.35768	0.59806	0.8846	-22.1	-22.3	-0.2
0.48758	0.69827	0.8516	-15.6	-15.8	-0.2
0.64129	0.80080	0.8169	-9.0	-9.2	-0.2
0.80241	0.89577	0.7844	-3.6	-3.2	0.4
0.98030	0.99010	0.7529	2.3	2.6	0.3
1.2070	1.0986	0.7185	9.4	9.2	-0.2
1.4501	1.2042	0.6863	15.2	15.3	0.1
1.7012	1.3043	0.6578	20.7	20.8	0.1
1.9673	1.4026	0.6319	26.0	26.0	0.0
2.2577	1.5026	0.6077	31.1	30.9	-0.2
2.5693	1.6029	0.5847	35.5	35.6	0.1
2.8997	1.7029	0.5641	39.8	39.9	0.1
3.2554	1.8043	0.5450	43.9	43.9	0.0
3.6100	1.9000	0.5282	47.3	47.2	-0.1
3.8271	1.9563	0.5187	49.0	49.0	0.0
4.2800[b]	2.0688	0.5012	52.3	52.3	0.0
				Average	±0.4

[a]Calculated from Equation 4.1 using coefficients given in Table 4.

[b]Saturated solution.

Table 7. Specific heat capacity and apparent molal heat capacity of aqueous $Tb(NO_3)_3$ solutions at 25°C

m	$m^{1/2}$	S_p cal/deg gm	Φ_{cp}	Φ_{cp} L.S.[a] cal/deg mole	Δ
0.087692	0.29613	0.9659	-43.1	-43.8	-0.7
0.15957	0.39946	0.9409	-38.9	-36.7	2.2
0.24577	0.49575	0.9141	-29.7	-30.2	-0.5
0.35351	0.59457	0.8830	-23.3	-23.5	-0.2
0.48247	0.69460	0.8496	-16.3	-16.7	-0.4
0.63136	0.79458	0.8151	-10.0	-10.2	-0.2
0.80016	0.89452	0.7804	-3.8	-3.7	0.1
0.97810	0.98899	0.7485	2.1	2.2	0.1
1.1872	1.0896	0.7155	8.1	8.3	0.2
1.4099	1.1874	0.6854	14.0	14.0	0.0
1.6596	1.2882	0.6560	19.6	19.6	0.0
1.9165	1.3844	0.6300	24.8	24.8	0.0
2.1903	1.4800	0.6059	29.6	29.6	0.0
2.4979	1.5805	0.5827	34.4	34.3	-0.1
2.8117	1.6768	0.5621	38.5	38.5	0.0
3.1449	1.7734	0.5431	42.4	42.4	0.0
3.5018	1.8713	0.5254	46.0	46.0	0.0
3.7529	1.9372	0.5141	48.2	48.2	0.0
4.1358[b]	2.0337	0.4989	51.2	51.2	0.0
4.5395[b]	2.1306	0.4845	53.8	53.8	0.0
				Average	±0.2

[a]Calculated from Equation 4.1 using coefficients given in Table 4.

[b]Saturated solution.

Table 8. Specific heat capacity and apparent molal heat capacity of aqueous $Dy(NO_3)_3$ solutions at 25°C

m	$m^{1/2}$	S_p cal/deg gm	Φ_{cp}	Φ_{cp}[a] L.S. cal/deg mole	Δ
0.091053	0.30175	0.9644	-42.9	-41.8	1.1
0.16470	0.40583	0.9391	-35.6	-35.5	0.1
0.25627	0.50623	0.9101	-29.2	-29.2	0.0
0.36965	0.60799	0.8776	-22.3	-22.5	-0.2
0.50497	0.71061	0.8428	-15.4	-15.7	-0.3
0.66019	0.81252	0.8073	-8.8	-8.9	-0.1
0.83776	0.91529	0.7716	-2.4	-2.1	0.3
1.0309	1.0153	0.7382	4.4	4.4	0.0
1.2508	1.1184	0.7051	10.9	10.8	-0.1
1.4887	1.2201	0.6743	16.9	16.9	0.0
1.7557	1.3250	0.6446	22.9	22.8	-0.1
2.0408	1.4286	0.6174	28.2	28.3	0.1
2.3480	1.5323	0.5923	33.3	33.3	0.0
2.6766	1.6360	0.5694	38.0	37.9	-0.1
3.0332	1.7416	0.5476	42.1	42.1	0.0
3.4037	1.8449	0.5283	45.8	45.8	0.0
3.8340	1.9581	0.5083	49.2	49.2	0.0
4.2666	2.0656	0.4910	52.1	52.1	0.0
4.7382[b]	2.1767	0.4742	54.5	54.5	0.0
				Average	±0.1

[a]Calculated from Equation 4.1 using coefficients given in Table 4.

[b]Saturated solution.

Table 9. Specific heat capacity and apparent molal heat capacity of aqueous $Ho(NO_3)_3$ solutions at 25°C

m	$m^{1/2}$	S_p cal/deg gm	Φ_{cp}	Φ_{cp} [a] L.S. cal/deg mole	Δ
0.099190	0.31494	0.9611	-44.2	-42.3	1.9
0.16815	0.41006	0.9372	-37.9	-36.6	1.3
0.25073	0.50073	0.9112	-30.1	-30.8	-0.7
0.35977	0.59981	0.8793	-23.9	-24.1	-0.2
0.49144	0.70103	0.8450	-16.7	-17.2	-0.5
0.54017	0.73496	0.8330	-14.8	-14.8	0.0
0.80190	0.89549	0.7771	-3.9	-3.8	0.1
0.99277	0.99638	0.7429	2.9	3.0	0.1
1.2098	1.0999	0.7094	9.7	9.8	0.1
1.4265	1.1944	0.6807	15.8	15.7	-0.1
1.6843	1.2978	0.6510	21.9	21.9	0.0
1.9571	1.3990	0.6238	27.2	27.4	0.2
2.2351	1.4950	0.6005	32.5	32.4	-0.1
2.5492	1.5966	0.5772	37.2	37.1	-0.1
2.8292	1.6820	0.5589	40.7	40.7	0.0
3.3331	1.8257	0.5312	46.1	46.0	-0.1
3.7182	1.9283	0.5126	49.1	49.2	0.1
4.1243	2.0308	0.4955	51.8	52.0	0.2
4.5568 [b]	2.1347	0.4800	54.6	54.4	-0.2
5.0183 [b]	2.2402	0.4641	56.3	56.4	0.1
				Average	±0.3

[a] Calculated from Equation 4.1 using coefficients given in Table 4.

[b] Saturated solution.

Table 10. Specific heat capacity and apparent molal heat capacity of aqueous $Tm(NO_3)_3$ solutions at 25°C

m	$m^{1/2}$	S_p cal/deg gm	Φ_{cp}	Φ_{cp} L.S.[a] cal/deg mole	Δ
0.091315	0.30218	0.9636	-44.7	-45.5	-0.8
0.16174	0.40217	0.9386	-40.0	-37.5	2.5
0.21439	0.46302	0.9219	-31.9	-33.0	-1.1
0.36021	0.60017	0.8783	-23.2	-23.2	0.0
0.47992	0.69276	0.8467	-16.7	-16.7	0.0
0.61645	0.78514	0.8145	-10.0	-10.1	-0.1
0.81942	0.90522	0.7730	-1.3	-1.3	0.0
0.99776	0.99888	0.7416	5.4	5.6	0.2
1.2105	1.1002	0.7097	13.0	13.0	0.0
1.4452	1.2022	0.6795	20.2	20.3	0.1
1.6965	1.3025	0.6523	27.2	27.1	-0.1
1.9611	1.4004	0.6272	33.1	33.2	0.1
2.2489	1.4996	0.6042	38.9	38.8	-0.1
2.5581	1.5994	0.5823	43.9	43.8	-0.1
2.9065	1.7048	0.5607	48.3	48.3	0.0
3.2464	1.8018	0.5418	51.5	51.6	0.1
3.7648	1.9403	0.5164	55.1	55.4	0.3
3.9972	1.9993	0.5068	56.8	56.6	-0.2
4.4117	2.1004	0.4897	58.4	58.3	-0.1
5.0157	2.2396	0.4675	60.0	59.9	-0.1
5.4573	2.3361	0.4524	60.4	60.7	0.3
5.9483[b]	2.4389	0.4383	61.3	61.3	0.0
				Average	±0.3

[a]Calculated from Equation 4.1 using coefficients given in Table 4.

[b]Saturated solution.

Table 11. Specific heat capacity and apparent molal heat capacity of aqueous $Yb(NO_3)_3$ solutions at 25°C

m	$m^{1/2}$	S_p cal/deg gm	Φ_{cp}	Φ_{cp} [a] L.S. cal/deg mole	Δ
0.094512	0.30743	0.9620	-45.6	-44.3	1.3
0.15922	0.39902	0.9394	-36.1	-37.2	-1.1
0.24679	0.49678	0.9107	-30.5	-30.3	0.2
0.35481	0.59566	0.8786	-23.7	-23.7	0.0
0.48259	0.69469	0.8446	-16.6	-16.9	-0.3
0.63307	0.79566	0.8085	-10.4	-9.9	0.5
0.79817	0.89340	0.7748	-2.6	-2.8	-0.2
0.98708	0.99352	0.7409	4.6	4.7	0.1
1.1939	1.0927	0.7095	12.4	12.2	-0.2
1.4164	1.1901	0.6804	19.5	19.5	0.0
1.6635	1.2898	0.6529	26.5	26.7	0.2
1.9253	1.3875	0.6285	33.3	33.3	0.0
2.2067	1.4855	0.6058	39.4	39.3	-0.1
2.5068	1.5833	0.5848	44.8	44.7	-0.1
2.8314	1.6827	0.5645	49.3	49.3	0.0
3.1642	1.7788	0.5460	52.9	53.0	0.1
3.5179	1.8756	0.5283	55.9	55.9	0.0
3.9024	1.9755	0.5104	58.1	58.2	0.1
4.2923	2.0718	0.4946	60.1	59.8	-0.3
4.7029	2.1686	0.4780	60.9	60.9	0.0
5.1302	2.2650	0.4628	61.7	61.7	0.0
5.5771	2.3616	0.4480	62.1	62.1	0.0
6.0413	2.4579	0.4344	62.5	62.5	0.0
6.5228	2.5540	0.4217	62.9	62.8	-0.1
6.6500[b]	2.5788	0.4181	62.8	62.8	0.0
				Average	±0.2

[a] Calculated from Equation 4.1 using coefficients given in Table 4.

[b] Saturated solution.

Table 12. Specific heat capacity and apparent molal heat capacity of aqueous $Pr(ClO_4)_3$ solutions at 25°C

m	$m^{1/2}$	S_p cal/deg gm	Φ_{cp}	Φ_{cp} [a] L.S. cal/deg mole	Δ
0.089236	0.29872	0.9585	-31.6	-29.2	2.4
0.15944	0.39930	0.9302	-22.4	-22.7	-0.3
0.24958	0.49958	0.8964	-17.0	-16.7	0.3
0.35703	0.59752	0.8600	-11.2	-11.3	-0.1
0.48814	0.69867	0.8199	-6.5	-6.1	0.4
0.63217	0.79509	0.7806	-2.3	-1.6	0.7
0.80157	0.89530	0.7406	3.1	2.8	-0.3
0.99104	0.99551	0.7011	7.4	7.0	-0.4
1.2004	1.0956	0.6630	11.4	10.9	-0.5
1.4242	1.1934	0.6274	14.8	14.5	-0.3
1.6698	1.2922	0.5936	18.1	18.1	0.0
1.9339	1.3907	0.5625	21.5	21.5	0.0
2.2219	1.4906	0.5333	24.7	25.0	0.3
2.5198	1.5874	0.5074	27.8	28.3	0.5
2.8444	1.6865	0.4838	31.4	31.8	0.4
3.1814	1.7837	0.4637	35.5	35.3	-0.2
3.5428	1.8822	0.4449	39.1	39.0	-0.1
3.6423	1.9085	0.4405	40.2	40.0	-0.2
3.9973	1.9993	0.4262	44.0	43.6	-0.4
4.4070	2.0993	0.4122	48.0	47.9	-0.1
4.6962[b]	2.1671	0.4036	50.5	50.9	0.4
				Average	±0.4

[a] Calculated from Equation 4.1 using coefficients given in Table 4.

[b] Saturated solution.

Table 13. Specific heat capacity and apparent molal heat capacity of aqueous $Sm(ClO_4)_3$ solutions at 25°C

m	$m^{1/2}$	S_p cal/deg gm	Φ_{cp}	Φ_{cp}[a] L.S. cal/deg mole	Δ
0.092050	0.30340	0.9569	-27.0	-25.2	1.8
0.16020	0.40025	0.9289	-19.9	-19.3	0.6
0.24913	0.49913	0.8953	-14.0	-13.6	0.4
0.35881	0.59901	0.8576	-9.0	-8.4	0.6
0.48671	0.69765	0.8184	-3.6	-3.6	0.0
0.63895	0.79934	0.7768	0.9	1.0	0.1
0.80385	0.89658	0.7374	5.5	5.2	-0.3
0.99739	0.99869	0.6966	9.5	9.2	-0.3
1.2095	1.0998	0.6580	13.4	13.1	-0.3
1.4388	1.1995	0.6217	16.8	16.7	-0.1
1.6828	1.2972	0.5885	20.2	20.2	0.0
1.9487	1.3960	0.5574	23.5	23.6	0.1
2.2445	1.4982	0.5278	27.0	27.2	0.2
2.5482	1.5963	0.5020	30.3	30.7	0.4
2.8832	1.6980	0.4786	34.3	34.4	0.1
3.2291	1.7970	0.4585	38.4	38.2	-0.2
3.5951	1.8961	0.4407	42.4	42.1	-0.3
3.9753	1.9938	0.4250	46.3	46.3	0.0
4.3237[b]	2.0794	0.4136	50.2	50.1	-0.1
4.6400[b]	2.1541	0.4045	53.4	53.7	0.3
				Average	±0.3

[a]Calculated from Equation 4.1 using coefficients given in Table 4.

[b]Saturated solution.

Table 14. Specific heat capacity and apparent molal heat capacity of aqueous $Tb(ClO_4)_3$ solutions at 25°C

m	$m^{1/2}$	S_p cal/deg gm	Φ_{cp}	Φ_{cp} [a] L.S. cal/deg mole	Δ
0.092736	0.30453	0.9565	-20.0	-17.8	2.2
0.16385	0.40478	0.9273	-12.9	-11.7	1.2
0.25177	0.50177	0.8943	-6.5	-6.3	0.2
0.36651	0.60540	0.8550	-1.6	-1.1	0.5
0.49239	0.70171	0.8165	2.9	3.3	0.4
0.64757	0.80472	0.7747	8.0	7.7	-0.3
0.82030	0.90570	0.7335	11.9	11.6	-0.3
1.0106	1.0053	0.6938	15.4	15.1	-0.3
1.2280	1.1081	0.6545	18.9	18.6	-0.3
1.4669	1.2112	0.6173	22.1	21.8	-0.3
1.7208	1.3118	0.5830	24.9	24.9	0.0
1.9958	1.4127	0.5511	27.6	27.8	0.2
2.2967	1.5155	0.5213	30.4	30.9	0.5
2.6136	1.6167	0.4946	33.3	33.9	0.6
2.9512	1.7179	0.4715	36.9	37.0	0.1
3.3151	1.8207	0.4507	40.7	40.2	-0.5
3.6998	1.9235	0.4316	44.1	43.7	-0.4
4.1078	2.0268	0.4148	47.5	47.5	0.0
4.3694[b]	2.0903	0.4058	49.8	50.0	0.2
4.6072[b]	2.1464	0.3989	52.1	52.3	0.2
				Average	±0.4

[a] Calculated from Equation 4.1 using coefficients given in Table 4.

[b] Saturated solution.

Table 15. Specific heat capacity and apparent molal heat capacity of aqueous $Dy(ClO_4)_3$ solutions at 25°C

m	$m^{1/2}$	S_p cal/deg gm	Φ_{cp}	Φ_{cp}[a] L.S. cal/deg mole	Δ
0.092683	0.30444	0.9565	-16.1	-16.6	-0.5
0.16134	0.40167	0.9281	-11.4	-10.9	0.5
0.24964	0.49964	0.8945	-5.8	-5.5	0.3
0.35844	0.59870	0.8569	-1.2	-0.6	0.6
0.48990	0.69993	0.8163	3.5	4.1	0.6
0.63986	0.79991	0.7756	8.4	8.3	-0.1
0.80781	0.89878	0.7350	12.1	12.2	0.1
0.99632	0.99816	0.6956	16.1	15.9	-0.2
1.2080	1.0991	0.6573	20.2	19.4	-0.8
1.4392	1.1997	0.6205	23.1	22.7	-0.4
1.6862	1.2985	0.5866	25.8	25.8	0.0
1.9577	1.3992	0.5544	28.4	28.8	0.4
2.2459	1.4986	0.5254	31.3	31.8	0.5
2.5571	1.5991	0.4986	34.1	34.7	0.6
2.8774	1.6963	0.4759	37.5	37.6	0.1
3.2341	1.7984	0.4544	41.1	40.8	-0.3
3.6006	1.8975	0.4355	44.3	43.9	-0.4
3.9929	1.9982	0.4182	47.3	47.2	-0.1
4.3542	2.0867	0.4050	50.2	50.3	0.1
4.6048[b]	2.1459	0.3970	52.3	52.5	0.2
				Average	±0.3

[a]Calculated from Equation 4.1 using coefficients given in Table 4.

[b]Saturated solution.

Table 16. Specific heat capacity and apparent molal heat capacity of aqueous $Ho(ClO_4)_3$ solutions at 25°C

m	$m^{1/2}$	S_p cal/deg gm	Φ_{cp}	Φ_{cp} [a] L.S. cal/deg mole	Δ
0.089489	0.29915	0.9576	-17.9	-15.1	2.8
0.16482	0.40598	0.9266	-9.3	-9.1	0.2
0.25718	0.50713	0.8915	-4.8	-3.8	1.0
0.37037	0.60858	0.8526	0.1	1.0	0.9
0.50543	0.71094	0.8115	5.3	5.6	0.3
0.66161	0.81339	0.7696	10.0	9.9	-0.1
0.83616	0.91442	0.7286	14.3	13.9	-0.4
1.0453	1.0224	0.6860	18.5	17.8	-0.7
1.2496	1.1179	0.6499	21.8	21.1	-0.7
1.4934	1.2221	0.6123	24.8	24.6	-0.2
1.7583	1.3260	0.5772	27.5	27.9	0.4
2.0480	1.4311	0.5449	30.7	31.1	0.4
2.3570	1.5353	0.5154	33.7	34.3	0.6
2.6449	1.6263	0.4923	36.5	37.0	0.5
3.0243	1.7391	0.4674	40.8	40.5	-0.3
3.4314	1.8524	0.4446	44.4	44.0	-0.4
3.8357	1.9585	0.4255	47.6	47.3	-0.3
4.2744	2.0675	0.4083	51.0	51.0	0.0
4.6241 [b]	2.1504	0.3966	53.5	53.8	0.3
				Average	±0.6

[a] Calculated from Equation 4.1 using coefficients given in Table 4.

[b] Saturated solution.

Table 17. Specific heat capacity and apparent molal heat capacity of aqueous $Er(ClO_4)_3$ solutions at 25°C

m	$m^{1/2}$	S_p cal/deg gm	Φ_{cp}	Φ_{cp} [a] L.S. cal/deg mole	Δ
0.096322	0.31036	0.9543	-19.1	-16.7	2.4
0.15929	0.39911	0.9284	-10.6	-11.3	-0.7
0.24856	0.49856	0.8938	-6.5	-5.8	0.7
0.35799	0.59832	0.8558	-1.2	-0.7	0.5
0.48624	0.69731	0.8159	3.5	4.0	0.5
0.63689	0.79805	0.7746	8.5	8.5	0.0
0.80895	0.89942	0.7331	12.8	12.6	-0.2
0.99727	0.99863	0.6936	16.8	16.4	-0.4
1.2006	1.0957	0.6562	20.1	19.9	-0.2
1.4352	1.1980	0.6193	23.8	23.3	-0.5
1.6812	1.2966	0.5853	26.5	26.5	0.0
1.9466	1.3952	0.5541	29.5	29.6	0.1
2.2439	1.4980	0.5239	32.3	32.8	0.5
2.5635	1.6011	0.4965	35.2	35.9	0.7
2.8609	1.6914	0.4758	38.7	38.7	0.0
3.2102	1.7917	0.4547	42.2	41.9	-0.3
3.5697	1.8894	0.4363	45.5	45.0	-0.5
3.9487	1.9871	0.4193	48.4	48.3	-0.1
4.3628	2.0887	0.4039	51.7	51.9	0.2
4.6185[b]	2.1491	0.3963	54.1	54.2	0.1
				Average	±0.4

[a] Calculated from Equation 4.1 using coefficients given in Table 4.

[b] Saturated solution.

Table 18. Specific heat capacity and apparent molal heat capacity of aqueous $Tm(ClO_4)_3$ solutions at 25°C

m	$m^{1/2}$	S_p cal/deg gm	Φ_{cp}	Φ_{cp} [a] L.S. cal/deg mole	Δ
0.089811	0.29968	0.9571	-18.1	-14.7	3.4
0.15891	0.39864	0.9286	-8.5	-9.3	-0.8
0.24747	0.49746	0.8942	-5.4	-4.3	1.1
0.35472	0.59558	0.8570	0.5	0.4	-0.1
0.48189	0.69418	0.8169	4.1	4.9	0.8
0.62977	0.79358	0.7760	8.6	9.1	0.5
0.80125	0.89513	0.7345	13.3	13.1	-0.2
0.98665	0.99330	0.6956	17.7	16.8	-0.9
1.1912	1.0914	0.6578	21.1	20.4	-0.7
1.4158	1.1899	0.6217	24.1	23.8	-0.3
1.6606	1.2886	0.5877	27.0	27.1	0.1
1.9186	1.3851	0.5570	30.0	30.3	0.3
2.2033	1.4844	0.5278	32.8	33.5	0.7
2.5034	1.5822	0.5018	35.9	36.6	0.7
2.8201	1.6793	0.4791	39.6	39.8	0.2
3.1582	1.7771	0.4590	43.5	43.0	-0.5
3.5135	1.8744	0.4401	46.6	46.2	-0.4
3.8817	1.9702	0.4235	49.7	49.5	-0.2
4.2753	2.0677	0.4088	53.0	53.0	0.0
4.5398	2.1307	0.3999	55.0	55.3	0.3
4.6172[b]	2.1488	0.3984	56.1	56.0	-0.1
				Average	±0.6

[a]Calculated from Equation 4.1 using coefficients given in Table 4.

[b]Saturated solution.

Table 19. Specific heat capacity and apparent molal heat capacity of aqueous $Yb(ClO_4)_3$ solutions at 25°C

m	$m^{1/2}$	S_p cal/deg gm	Φ_{cp}	Φ_{cp} L.S.[a] cal/deg mole	Δ
0.099350	0.31520	0.9524	-18.9	-18.1	0.8
0.15879	0.39848	0.9272	-14.5	-12.9	1.6
0.24803	0.49803	0.8918	-11.2	-7.2	4.0
0.35709	0.59757	0.8545	-1.7	-1.9	-0.2
0.49385	0.70274	0.8115	3.0	3.3	0.3
0.63974	0.79984	0.7715	8.2	7.7	-0.5
0.81122	0.90068	0.7300	12.6	12.1	-0.5
1.0012	1.0006	0.6900	16.8	16.1	-0.7
1.2121	1.1010	0.6514	20.4	19.9	-0.5
1.4396	1.1998	0.6153	23.5	23.4	-0.1
1.6845	1.2979	0.5820	26.8	26.8	0.0
1.9622	1.4008	0.5494	29.9	30.2	0.3
2.2475	1.4992	0.5208	32.7	33.4	0.7
2.5528	1.5978	0.4947	35.7	36.5	0.8
2.8893	1.6998	0.4716	39.8	39.8	0.0
3.2390	1.7997	0.4509	43.4	43.0	-0.4
3.6087	1.8997	0.4323	46.7	46.3	-0.4
3.9893	1.9973	0.4154	49.6	49.5	-0.1
4.1563[b]	2.0387	0.4095	51.2	51.0	-0.2
4.6044[b]	2.1458	0.3939	54.3	54.8	0.5
				Average	±0.6

[a]Calculated from Equation 4.1 using coefficients given in Table 4.

[b]Saturated solution.

Table 20. Apparent molal heat capacity of aqueous $RE(NO_3)_3$ solutions at even molalities and 25°C

m	Φ_{cp} (cal/deg mole) $La(NO_3)_3$[a]	$Pr(NO_3)_3$	$Nd(NO_3)_3$[a]	$Sm(NO_3)_3$	$Gd(NO_3)_3$[a]	$Tb(NO_3)_3$
0.2	-36.8	-36.3	-33.9	-32.1	-31.2	-33.5
0.4	-22.7	-22.0	-20.7	-20.1	-19.6	-20.9
0.6	-12.0	-11.6	-10.8	-10.9	-10.7	-11.5
0.8	-3.2	-3.1	-2.8	-3.3	-3.4	-3.7
1.0	4.1	4.1	4.1	3.2	3.0	2.9
1.2	10.4	10.2	10.1	9.0	8.6	8.6
1.4	15.9	15.6	15.4	14.1	13.6	13.8
1.6	20.7	20.4	20.1	18.7	18.1	18.4
1.8	25.0	24.7	24.3	22.8	22.3	22.5
2.0	28.7	28.5	28.2	26.6	26.0	26.3
2.2	32.1	32.0	31.7	30.0	29.5	29.7
2.4	35.1	35.1	34.8	33.2	32.6	32.8
2.6	37.8	38.0	37.7	36.0	35.5	35.7
2.8	40.2	40.6	40.3	38.6	38.2	38.4
3.0	42.4	42.9	42.7	41.1	40.6	40.8
3.2	44.4	45.1	44.9	43.3	42.8	43.0
3.4	46.1	47.0	46.8	45.3	44.8	45.0
3.6	47.7	48.8	48.6	47.1	46.6	46.9
3.8	49.2	50.5	50.2	48.8	48.3	48.6
4.0	50.5	52.0	51.7	50.4	49.7	50.2
4.2	51.7	53.4	53.0	51.8	51.1	51.6
4.4	52.8	54.6	54.1		52.2	52.9
4.6	53.8	55.7	55.1			
4.8		56.8				
5.0		57.7				

[a]Results obtained by Walters (16).

Table 20. (Continued)

m	Φ_{cp} (cal/deg mole) $Dy(NO_3)_3$	$Ho(NO_3)_3$	$Er(NO_3)_3$[a]	$Tm(NO_3)_3$	$Yb(NO_3)_3$	$Lu(NO_3)_3$[a]
0.2	-32.9	-34.2	-33.3	-34.1	-33.7	-34.8
0.4	-20.9	-21.9	-21.8	-21.0	-21.2	-21.8
0.6	-11.4	-12.1	-11.9	-10.9	-11.4	-12.3
0.8	-3.4	-3.8	-3.2	-2.1	-2.7	-3.8
1.0	3.4	3.3	4.4	5.7	5.2	4.1
1.2	9.4	9.5	11.1	12.7	12.4	11.5
1.4	14.7	15.0	17.0	18.9	19.0	18.3
1.6	19.5	20.0	22.2	24.6	24.9	24.6
1.8	23.7	24.3	26.8	29.6	30.2	30.3
2.0	27.5	28.2	30.9	34.0	35.0	35.3
2.2	31.0	31.8	34.5	37.9	39.2	39.8
2.4	34.1	34.9	37.6	41.4	42.9	43.8
2.6	36.9	37.8	40.4	44.4	46.1	47.2
2.8	39.5	40.3	42.9	47.0	48.9	50.2
3.0	41.8	42.6	45.0	49.3	51.3	52.6
3.2	43.8	44.7	46.9	51.2	53.3	54.7
3.4	45.7	46.6	48.6	52.9	55.0	56.4
3.6	47.5	48.3	50.1	54.3	56.5	57.8
3.8	49.0	49.8	51.4	55.6	57.7	59.0
4.0	50.4	51.2	52.5	56.6	58.7	59.8
4.2	51.7	52.4	53.5	57.5	59.5	60.5
4.4	52.8	53.6	54.4	58.2	60.2	61.0
4.6	53.8	54.6	55.3	58.9	60.7	61.4
4.8		55.5	56.0	59.4	61.1	61.6
5.0		56.3	56.7	59.9	61.5	61.8
5.2			57.4	60.3	61.8	61.8
5.4			58.1	60.6	62.0	61.9
5.6				60.9	62.2	61.9
5.8				61.1	62.3	62.0
6.0					62.5	62.0
6.2					62.6	62.0
6.4					62.7	62.0
6.6					62.8	62.1
6.8						62.1

Table 21. Partial molal heat capacity of the solvent for aqueous $RE(NO_3)_3$ solutions at even molalities and 25°C

m	$\bar{C}_{pl}$ (cal/deg mole)					
	$La(NO_3)_3$[a]	$Pr(NO_3)_3$	$Nd(NO_3)_3$[a]	$Sm(NO_3)_3$	$Gd(NO_3)_3$[a]	$Tb(NO_3)_3$
0.2	17.934	17.933	17.938	17.943	17.945	17.940
0.4	17.822	17.824	17.835	17.847	17.853	17.842
0.6	17.685	17.693	17.709	17.727	17.737	17.721
0.8	17.537	17.550	17.569	17.592	17.604	17.586
1.0	17.385	17.401	17.420	17.446	17.460	17.441
1.2	17.235	17.250	17.268	17.296	17.309	17.292
1.4	17.090	17.100	17.115	17.143	17.154	17.141
1.6	16.953	16.955	16.964	16.991	17.000	16.991
1.8	16.827	16.815	16.818	16.843	16.848	16.844
2.0	16.713	16.683	16.680	16.700	16.700	16.702
2.2	16.610	16.559	16.550	16.565	16.561	16.566
2.4	16.521	16.445	16.432	16.438	16.431	16.439
2.6	16.444	16.342	16.325	16.322	16.313	16.321
2.8	16.379	16.249	16.233	16.217	16.209	16.214
3.0	16.325	16.167	16.155	16.125	16.121	16.117
3.2	16.282	16.097	16.093	16.046	16.050	16.033
3.4	16.248	16.038	16.049	15.982	15.999	15.963
3.6	16.222	15.991	16.022	15.934	15.969	15.905
3.8	16.202	15.956	16.015	15.901	15.962	15.862
4.0	16.186	15.931	16.027	15.885	15.980	15.834
4.2	16.173	15.918	16.060	15.886	16.024	15.822
4.4	16.160	15.915	16.114		16.096	15.825
4.6	16.146	15.923	16.191			
4.8		15.940				
5.0		15.966				

[a]Results obtained by Walters (16).

Table 21. (Continued)

m	$Dy(NO_3)_3$	$Ho(NO_3)_3$	$Er(NO_3)_3$[a]	$Tm(NO_3)_3$	$Yb(NO_3)_3$	$Lu(NO_3)_3$[a]
			$\overline{C}_{pl}$ (cal/deg mole)			
0.2	17.945	17.944	17.951	17.936	17.939	17.932
0.4	17.844	17.840	17.842	17.835	17.842	17.845
0.6	17.716	17.706	17.694	17.693	17.699	17.708
0.8	17.572	17.555	17.528	17.521	17.519	17.524
1.0	17.419	17.396	17.354	17.331	17.316	17.307
1.2	17.264	17.236	17.182	17.136	17.103	17.074
1.4	17.110	17.078	17.018	16.947	16.894	16.840
1.6	16.962	16.928	16.868	16.772	16.699	16.620
1.8	16.820	16.787	16.736	16.618	16.528	16.427
2.0	16.689	16.658	16.622	16.491	16.386	16.270
2.2	16.569	16.542	16.529	16.393	16.279	16.155
2.4	16.461	16.440	16.456	16.324	16.207	16.085
2.6	16.366	16.352	16.404	16.286	16.171	16.062
2.8	16.284	16.279	16.370	16.275	16.170	16.084
3.0	16.217	16.220	16.354	16.290	16.202	16.147
3.2	16.163	16.176	16.353	16.327	16.263	16.248
3.4	16.123	16.144	16.364	16.382	16.349	16.381
3.6	16.096	16.124	16.385	16.452	16.454	16.538
3.8	16.082	16.116	16.411	16.532	16.573	16.713
4.0	16.079	16.117	16.439	16.618	16.701	16.897
4.2	16.087	16.126	16.465	16.707	16.832	17.084
4.4	16.105	16.141	16.484	16.796	16.962	17.264
4.6	16.132	16.160	16.491	16.882	17.085	17.433
4.8		16.182	16.481	16.964	17.198	17.583
5.0		16.204	16.449	17.042	17.297	17.710
5.2			16.389	17.117	17.381	17.810
5.4			16.296	17.190	17.448	17.882
5.6				17.265	17.498	17.926
5.8				17.349	17.534	17.942
6.0					17.559	17.937
6.2					17.578	17.915
6.4					17.597	17.887
6.6					17.627	17.864
6.8						17.862

Table 22. Partial molal heat capacity of the solute for aqueous $RE(NO_3)_3$ solutions at even molalities and 25°C

m	$\bar{C}_{p2}$ (cal/deg mole)					
	$La(NO_3)_3$[a]	$Pr(NO_3)_3$	$Nd(NO_3)_3$[a]	$Sm(NO_3)_3$	$Gd(NO_3)_3$[a]	$Tb(NO_3)_3$
0.2	-19.8	-18.8	-17.8	-17.6	-17.2	-18.2
0.4	1.5	1.8	1.5	0.5	0.2	0.3
0.6	16.8	16.4	15.6	13.9	13.2	13.9
0.8	28.6	27.8	26.8	24.7	23.8	24.7
1.0	38.0	37.1	36.0	33.7	32.7	33.6
1.2	45.6	44.7	43.8	41.4	40.4	41.2
1.4	51.8	51.1	50.3	47.9	47.0	47.7
1.6	56.9	56.5	55.9	53.5	52.7	53.2
1.8	61.0	61.1	60.6	58.4	57.7	58.0
2.0	64.4	64.9	64.7	62.5	62.0	62.2
2.2	67.0	68.2	68.1	66.1	65.7	65.8
2.4	69.2	71.0	71.0	69.2	68.8	68.8
2.6	70.9	73.3	73.4	71.8	71.4	71.5
2.8	72.3	75.2	75.3	73.9	73.6	73.7
3.0	73.3	76.7	76.8	75.7	75.3	75.5
3.2	74.1	78.0	77.9	77.1	76.5	77.0
3.4	74.6	79.0	78.6	78.2	77.4	78.2
3.6	75.1	79.7	79.0	78.9	77.9	79.1
3.8	75.4	80.3	79.2	79.4	78.0	79.8
4.0	75.6	80.6	79.0	79.7	77.7	80.2
4.2	75.8	80.8	78.5	79.6	77.1	80.4
4.4	75.9	80.8	77.8		76.2	80.3
4.6	76.1	80.8	76.9			
4.8		80.5				
5.0		80.2				

[a]Results obtained by Walters (16).

Table 22. (Continued)

m	$Dy(NO_3)_3$	$Ho(NO_3)_3$	$Er(NO_3)_3$[a]	$Tm(NO_3)_3$	$Yb(NO_3)_3$	$Lu(NO_3)_3$[a]
			$\bar{C}_{p2}$ (cal/deg mole)			
0.2	-18.8	-20.0	-21.0	-17.8	-18.1	-17.2
0.4	0.1	-0.3	-0.5	1.3	0.2	-0.8
0.6	14.4	14.7	16.0	17.1	16.1	14.3
0.8	25.9	26.7	29.3	30.8	30.4	28.9
1.0	35.4	36.6	40.1	42.5	43.0	42.3
1.2	43.2	44.7	48.8	52.4	53.7	54.2
1.4	49.8	51.4	55.8	60.5	62.7	64.2
1.6	55.3	57.0	61.3	67.0	69.9	72.3
1.8	60.0	61.6	65.7	72.0	75.5	78.6
2.0	63.8	65.4	69.0	75.8	79.6	83.2
2.2	67.0	68.4	71.5	78.4	82.5	86.3
2.4	69.6	70.9	73.2	80.0	84.2	88.0
2.6	71.7	72.9	74.4	80.9	85.0	88.5
2.8	73.4	74.4	75.1	81.1	85.1	88.1
3.0	74.7	75.5	75.4	80.8	84.4	86.8
3.2	75.6	76.3	75.4	80.2	83.4	85.0
3.4	76.3	76.8	75.2	79.2	81.9	82.8
3.6	76.8	77.1	74.9	78.2	80.3	80.3
3.8	77.0	77.3	74.5	77.0	78.5	77.7
4.0	77.0	77.3	74.1	75.7	76.6	75.1
4.2	76.9	77.1	73.8	74.5	74.9	72.6
4.4	76.6	76.9	73.5	73.4	73.2	70.2
4.6	76.3	76.7	73.4	72.3	71.7	68.1
4.8		76.4	73.6	71.3	70.4	66.4
5.0		76.2	73.9	70.4	69.2	64.9
5.2			74.6	69.6	68.3	63.8
5.4			75.5	68.9	67.6	63.1
5.6				68.1	67.1	62.6
5.8				67.3	66.8	62.5
6.0					66.5	62.5
6.2					66.4	62.7
6.4					66.2	63.0
6.6					65.9	63.2
6.8						63.2

Table 23. Apparent molal heat capacity of aqueous $RE(ClO_4)_3$ solutions at even molalities and 25°C

m	Φ_{cp} (cal/deg mole)					
	La $(ClO_4)_3$[a]	Pr $(ClO_4)_3$	Nd $(ClO_4)_3$[a]	Sm $(ClO_4)_3$	Gd $(ClO_4)_3$[a]	Tb $(ClO_4)_3$
0.2	-18.3	-19.8	-19.3	-16.5	-11.6	-9.3
0.4	-8.2	-9.5	-8.5	-6.7	-2.2	0.2
0.6	-1.5	-2.5	-1.4	-0.1	4.0	6.4
0.8	3.7	2.8	4.1	5.1	8.7	11.2
1.0	7.9	7.2	8.4	9.3	12.5	15.0
1.2	11.4	10.9	12.1	12.9	15.8	18.2
1.4	14.5	14.2	15.3	16.1	18.6	21.0
1.6	17.3	17.1	18.2	19.0	21.2	23.5
1.8	19.8	19.8	20.8	21.7	23.5	25.8
2.0	22.1	22.3	23.3	24.3	25.7	27.9
2.2	24.3	24.7	25.6	26.7	27.8	29.9
2.4	26.4	27.0	27.7	29.0	29.8	31.9
2.6	28.4	29.2	29.8	31.3	31.8	33.7
2.8	30.3	31.3	31.9	33.5	33.7	35.6
3.0	32.2	33.4	33.9	35.7	35.6	37.4
3.2	34.0	35.5	35.9	37.9	37.5	39.2
3.4	35.8	37.5	37.8	40.0	39.4	41.0
3.6	37.6	39.6	39.8	42.2	41.3	42.8
3.8	39.4	41.6	41.8	44.4	43.2	44.6
4.0	41.2	43.7	43.8	46.5	45.2	46.5
4.2	43.0	45.7	45.8	48.7	47.1	48.4
4.4	44.8	47.8	47.8	51.0	49.1	50.3
4.6	46.6	49.9	49.8	53.2	51.1	52.2
4.8	48.4					

[a]Results obtained by Walters (16).

Table 23. (Continued)

m	Φ_{cp} (cal/deg mole)					
	$Dy(ClO_4)_3$	$Ho(ClO_4)_3$	$Er(ClO_4)_3$	$Tm(ClO_4)_3$	$Yb(ClO_4)_3$	$Lu(ClO_4)_3$[a]
0.2	-8.3	-6.9	-8.6	-6.8	-10.1	-9.6
0.4	1.0	2.2	1.0	2.1	-0.2	0.3
0.6	7.3	8.3	7.5	8.3	6.6	7.0
0.8	12.1	13.1	12.4	13.1	11.8	12.1
1.0	16.0	17.0	16.4	17.1	16.0	16.2
1.2	19.3	20.4	19.8	20.5	19.7	19.8
1.4	22.2	23.3	22.8	23.6	22.8	22.8
1.6	24.7	26.0	25.5	26.3	25.7	25.6
1.8	27.1	28.4	28.0	28.9	28.3	28.0
2.0	29.3	30.6	30.2	31.2	30.7	30.3
2.2	31.3	32.7	32.4	33.4	32.9	32.4
2.4	33.3	34.7	34.4	35.6	35.0	34.4
2.6	35.1	36.6	36.3	37.6	37.0	36.3
2.8	37.0	38.5	38.2	39.6	39.0	38.2
3.0	38.7	40.2	40.0	41.5	40.8	39.9
3.2	40.5	42.0	41.8	43.4	42.6	41.6
3.4	42.2	43.7	43.6	45.2	44.4	43.3
3.6	43.9	45.4	45.3	47.0	46.2	44.9
3.8	45.6	47.0	47.0	48.8	47.9	46.5
4.0	47.3	48.7	48.8	50.6	49.6	48.1
4.2	49.0	50.3	50.5	52.4	51.3	49.7
4.4	50.7	52.0	52.3	54.1	53.0	51.3
4.6	52.4	53.6	54.0	55.9	54.7	52.9

Table 24. Partial molal heat capacity of the solvent for aqueous $RE(ClO_4)_3$ solutions at even molalities and 25°C

m	$\overline{C}_{pl}$ (cal/deg mole)					
	La $(ClO_4)_3$[a]	Pr $(ClO_4)_3$	Nd $(ClO_4)_3$[a]	Sm $(ClO_4)_3$	Gd $(ClO_4)_3$[a]	Tb $(ClO_4)_3$
0.2	17.948	17.947	17.944	17.950	17.951	17.951
0.4	17.881	17.878	17.873	17.883	17.889	17.889
0.6	17.807	17.802	17.797	17.809	17.823	17.822
0.8	17.731	17.721	17.718	17.730	17.753	17.754
1.0	17.651	17.635	17.636	17.646	17.681	17.683
1.2	17.568	17.545	17.551	17.555	17.604	17.609
1.4	17.481	17.449	17.461	17.457	17.521	17.530
1.6	17.389	17.346	17.365	17.350	17.432	17.444
1.8	17.291	17.234	17.261	17.233	17.333	17.351
2.0	17.184	17.113	17.148	17.104	17.224	17.248
2.2	17.069	16.980	17.024	16.963	17.103	17.133
2.4	16.944	16.835	16.887	16.806	16.968	17.006
2.6	16.807	16.676	16.735	16.633	16.817	16.864
2.8	16.657	16.501	16.567	16.442	16.649	16.705
3.0	16.493	16.310	16.381	16.232	16.462	16.529
3.2	16.314	16.100	16.176	16.000	16.254	16.332
3.4	16.117	15.870	15.950	15.747	16.024	16.115
3.6	15.903	15.619	15.701	15.469	15.770	15.875
3.8	15.669	15.346	15.428	15.167	15.492	15.610
4.0	15.414	15.049	15.129	14.838	15.186	15.320
4.2	15.138	14.727	14.802	14.480	14.852	15.002
4.4	14.839	14.378	14.447	14.094	14.488	14.656
4.6	14.516	14.002	14.062	13.677	14.094	14.279
4.8	14.167					

[a]Results obtained by Walters (16).

Table 24. (Continued)

m	$\bar{C}_{pl}$ (cal/deg mole)					
	$Dy(ClO_4)_3$	$Ho(ClO_4)_3$	$Er(ClO_4)_3$	$Tm(ClO_4)_3$	$Yb(ClO_4)_3$	$Lu(ClO_4)_3$[a]
0.2	17.952	17.954	17.951	17.954	17.949	17.949
0.4	17.889	17.892	17.886	17.892	17.882	17.882
0.6	17.821	17.822	17.815	17.822	17.806	17.809
0.8	17.749	17.748	17.741	17.746	17.727	17.732
1.0	17.675	17.671	17.664	17.664	17.644	17.653
1.2	17.597	17.590	17.583	17.577	17.558	17.571
1.4	17.516	17.504	17.498	17.485	17.467	17.486
1.6	17.429	17.414	17.407	17.387	17.372	17.397
1.8	17.336	17.317	17.311	17.282	17.272	17.304
2.0	17.235	17.214	17.207	17.169	17.165	17.206
2.2	17.126	17.104	17.094	17.048	17.051	17.101
2.4	17.006	16.986	16.972	16.918	16.928	16.988
2.6	16.876	16.857	16.838	16.778	16.797	16.867
2.8	16.732	16.719	16.692	16.626	16.655	16.736
3.0	16.575	16.570	16.533	16.463	16.501	16.595
3.2	16.404	16.408	16.359	16.288	16.336	16.442
3.4	16.215	16.233	16.169	16.099	16.157	16.277
3.6	16.010	16.044	15.962	15.895	15.964	16.098
3.8	15.786	15.840	15.737	15.676	15.755	15.904
4.0	15.542	15.620	15.493	15.441	15.530	15.695
4.2	15.277	15.384	15.228	15.190	15.288	15.469
4.4	14.990	15.130	14.941	14.920	15.028	15.225
4.6	14.680	14.857	14.632	14.632	14.748	14.963

Table 25. Partial molal heat capacity of the solute for aqueous $RE(ClO_4)_3$ solutions at even molalities and 25°C

m	$\bar{C}_{p2}$ (cal/deg mole)					
	La $(ClO_4)_3$[a]	Pr $(ClO_4)_3$	Nd $(ClO_4)_3$[a]	Sm $(ClO_4)_3$	Gd $(ClO_4)_3$[a]	Tb $(ClO_4)_3$
0.2	-5.2	-6.4	-5.2	-3.8	0.7	3.2
0.4	7.7	6.8	8.4	8.9	12.5	15.0
0.6	15.9	15.4	17.0	17.2	20.0	22.4
0.8	22.1	21.9	23.3	23.5	25.5	27.9
1.0	27.0	27.1	28.4	28.7	30.0	32.3
1.2	31.2	31.7	32.7	33.3	33.9	36.0
1.4	34.9	35.8	36.5	37.5	37.4	39.4
1.6	38.3	39.6	40.1	41.4	40.7	42.6
1.8	41.5	43.3	43.5	45.3	44.0	45.6
2.0	44.6	46.8	46.8	49.0	47.2	48.6
2.2	47.7	50.3	50.1	52.8	50.4	51.7
2.4	50.7	53.8	53.4	56.5	53.6	54.8
2.6	53.7	57.4	56.8	60.4	57.0	57.9
2.8	56.8	61.0	60.2	64.3	60.4	61.2
3.0	60.0	64.6	63.8	68.3	64.0	64.5
3.2	63.2	68.4	67.4	72.5	67.7	68.0
3.4	66.5	72.2	71.2	76.7	71.6	71.7
3.6	69.9	76.2	75.2	81.1	75.6	75.5
3.8	73.4	80.3	79.3	85.7	79.8	79.5
4.0	77.0	84.6	83.5	90.4	84.1	83.6
4.2	80.7	88.9	88.0	95.2	88.6	87.9
4.4	84.6	93.4	92.5	100.2	93.4	92.4
4.6	88.6	98.0	97.3	105.3	98.2	97.0
4.8	92.7					

[a]Results obtained by Walters (16).

Table 25. (Continued)

m	$\bar{C}_{p2}$ (cal/deg mole)					
	$Dy(ClO_4)_3$	$Ho(ClO_4)_3$	$Er(ClO_4)_3$	$Tm(ClO_4)_3$	$Yb(ClO_4)_3$	$Lu(ClO_4)_3$[a]
0.2	3.8	4.8	3.9	4.6	2.7	3.2
0.4	15.8	16.6	16.2	16.4	15.6	16.0
0.6	23.4	24.4	24.1	24.3	24.1	24.2
0.8	29.2	30.2	30.1	30.4	30.4	30.4
1.0	33.8	35.0	34.8	35.5	35.6	35.3
1.2	37.7	39.1	38.9	39.9	39.9	39.4
1.4	41.2	42.8	42.6	43.8	43.8	43.0
1.6	44.4	46.2	45.9	47.4	47.3	46.3
1.8	47.4	49.3	49.1	50.9	50.6	49.4
2.0	50.4	52.3	52.1	54.2	53.7	52.2
2.2	53.3	55.2	55.1	57.4	56.7	55.0
2.4	56.2	58.1	58.0	60.5	59.7	57.8
2.6	59.0	60.9	61.0	63.6	62.6	60.4
2.8	62.0	63.8	64.0	66.7	65.5	63.1
3.0	65.0	66.6	67.1	69.8	68.5	65.8
3.2	68.1	69.5	70.2	73.0	71.4	68.6
3.4	71.2	72.5	73.4	76.2	74.4	71.3
3.6	74.5	75.5	76.6	79.4	77.5	74.2
3.8	77.9	78.5	80.0	82.7	80.6	77.1
4.0	81.3	81.6	83.5	86.0	83.8	80.1
4.2	84.9	84.8	87.1	89.4	87.1	83.1
4.4	88.6	88.1	90.8	92.9	90.5	86.3
4.6	92.4	91.5	94.6	96.5	93.9	89.5

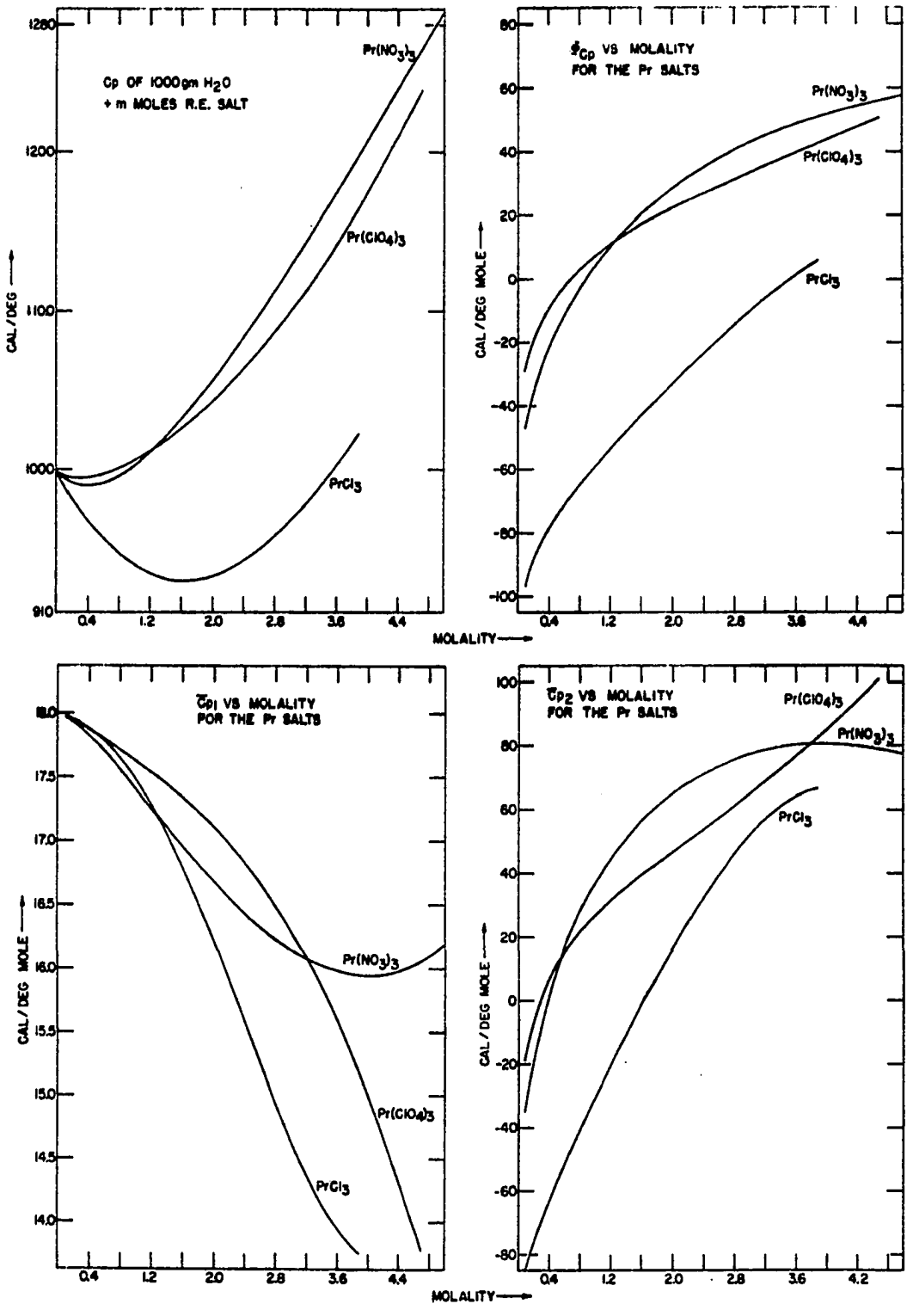

Figure 4. Heat capacity properties of $Pr(NO_3)_3$, $Pr(ClO_4)_3$ and $PrCl_3$ solutions at 25°C

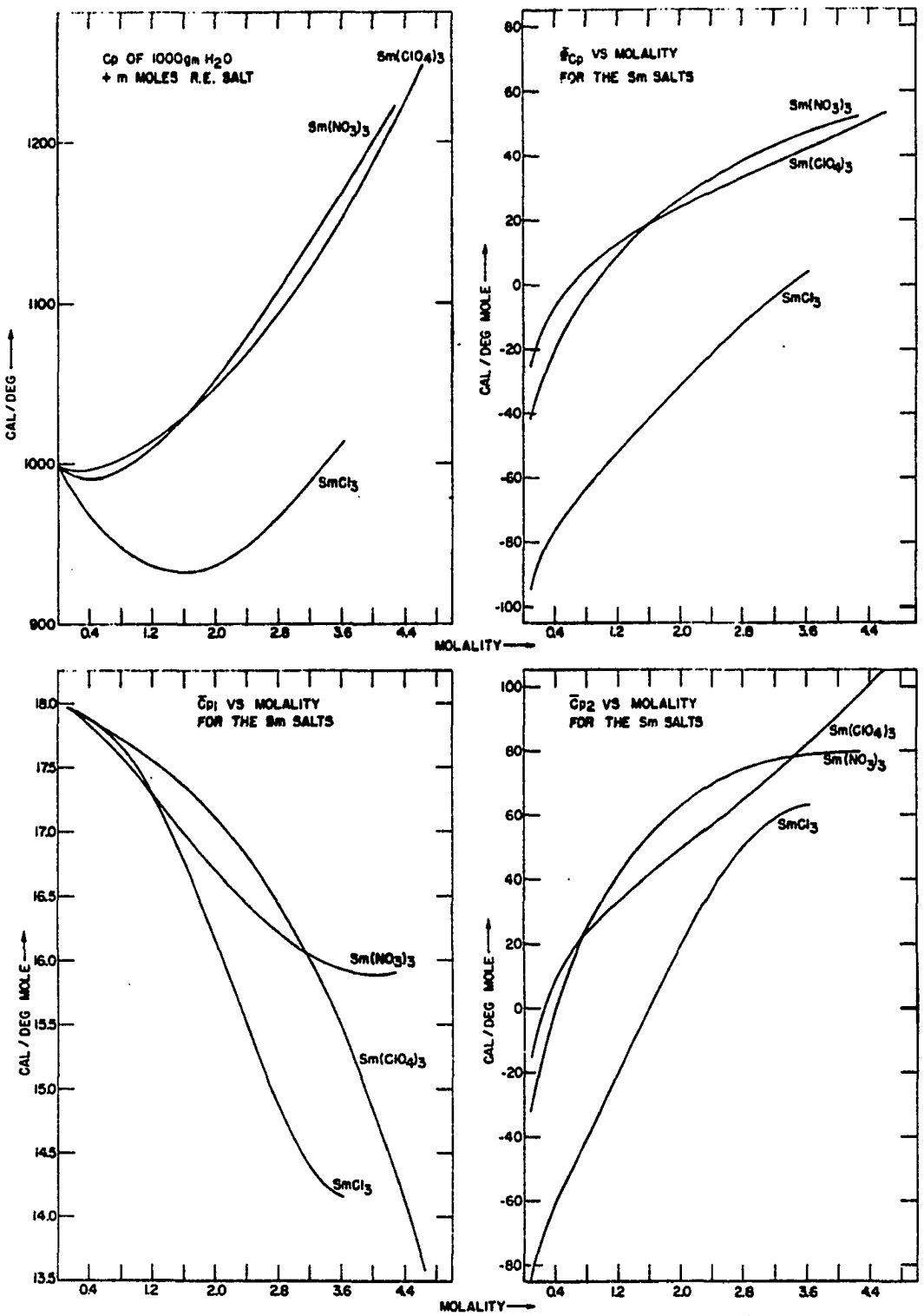

Figure 5. Heat capacity properties of $Sm(NO_3)_3$, $Sm(ClO_4)_3$ and $SmCl_3$ solutions at 25°C

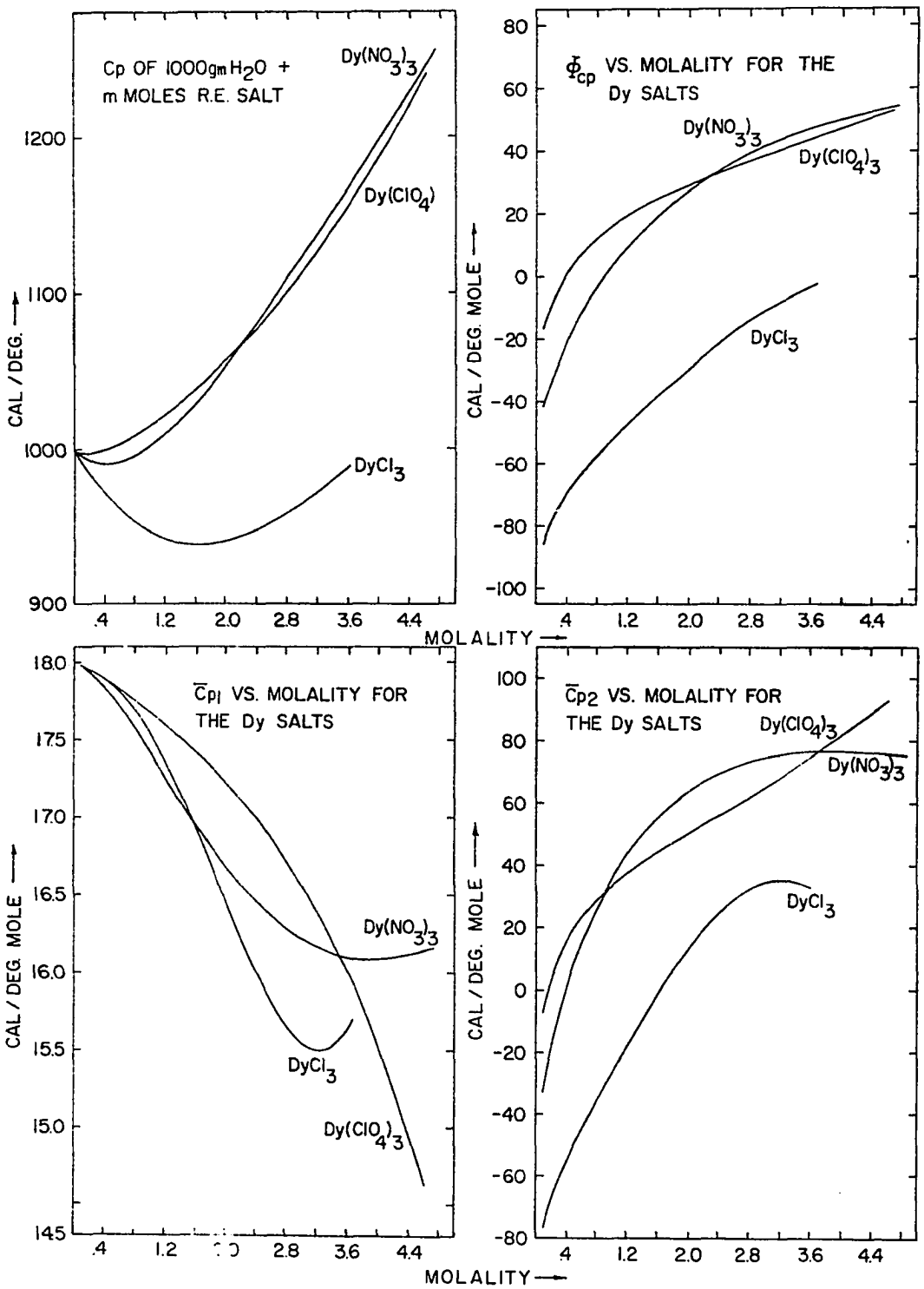

Figure 6. Heat capacity properties of $Dy(NO_3)_3$, $Dy(ClO_4)_3$ and $DyCl_3$ solutions at 25°C

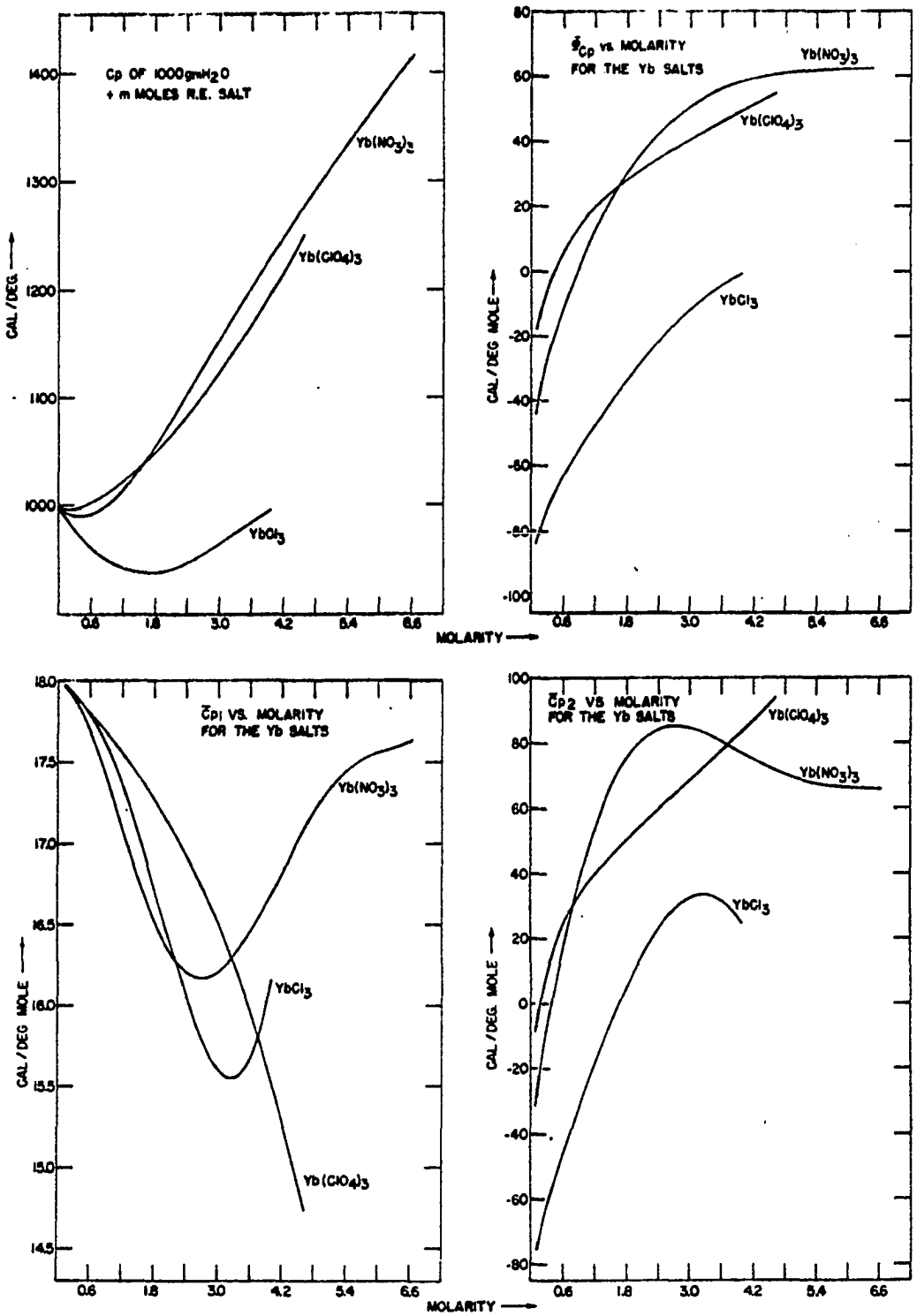

Figure 7. Heat capacity properties of $Yb(NO_3)_3$, $Yb(ClO_4)_3$ and $YbCl_3$ solutions at 25°C

propagation of precision indices (34) could then be used to estimate the probable error in Φ_{cp}. For Φ_{cp} (m,S_p) this principle states

$$P_{\Phi_{cp}} = \left[\left(\frac{\partial \Phi_{cp}}{\partial m} \right)^2_{S_p} P_m^2 + \left(\frac{\partial \Phi_{cp}}{\partial S_p} \right)^2_{m} P_{S_p}^2 \right]^{1/2} \qquad (4.4)$$

where P symbolizes probable error and the subscripts refer to the variables in question. Carrying out the differentiation of Equation 4.4 on Equation 2.11 results in

$$P_{\Phi_{cp}} = \left[\left(\frac{1,000}{m^2} (S_p^\circ - S_p) \right)^2 P_m^2 + \left(\frac{1,000}{m} + M_2 \right)^2 P_{S_p}^2 \right]^{1/2} \qquad (4.5)$$

The probable error in the specific heat capacity, P_{S_p}, was taken to be 0.05% of S_p, the same as the assumed accuracy. The probable error in the molality, P_m, for the stock and saturated solutions was taken to be 0.1% of their molality from the precision of the analyses made on these solutions. The concentrations, m, of the more dilute solutions prepared by weight from the stock solution were calculated from

$$m = \frac{1,000\ m' W_s}{1,000\ W_s + W_h\ (m' M_2 + 1,000)} \qquad (4.6)$$

where m' is the molality of the stock solution, M_2 is the molecular weight of the solute, W_s is the weight of stock solution used, and W_h is the weight of water used. The

probable error in m, P_m, assuming, as was alluded to in the experimental section, that weighing errors are negligible compared to analytical errors, is given by

$$P_m = \frac{\partial m}{\partial m'} P_{m'}$$

where $P_{m'}$ is the probable error in the molality of the stock solution, i.e., 0.1% of m'. Performing the differentiation on Equation 4.6 yields

$$P_m = \frac{(1{,}000)^2 (W_s^2 + W_s W_h)}{[1{,}000\ W_s + W_h\ (m'M_2 + 1{,}000)]^2} P_{m'}, \qquad (4.7)$$

Equation 4.7 was used to estimate probable errors in concentration, P_m, in order that the probable errors in Φ_{cp}, $P_{\Phi_{cp}}$, could be estimated from Equation 4.5.

The probable errors estimated for $Sm(NO_3)_3$ and $Sm(ClO_4)_3$ solutions are listed in Tables 26 and 27. It is apparent upon examination of Equations 4.6 and 4.7 and Tables 26 and 27 that as the ratio of W_s/W_h decreases (i.e., the solutions become more dilute) the probable error in molality, P_m, decreases faster than the molality, m. It is also apparent from Tables 26 and 27 that for the less concentrated solutions (below two molal) probable error in the specific heat capacity is the dominant factor in determining $P_{\Phi_{cp}}$.

The error in Φ_{cp} caused by a 0.1% error in the molality of the stock solution is essentially a constant for all the solutions prepared from the stock solution. This can be seen

Table 26. Probable error in molality and in the apparent molal heat capacity for $Sm(NO_3)_3$ solutions

m	P_m	$\Phi_{cp}{}^a$	Δ^b	$\left(\frac{\partial \Phi_{cp}}{\partial m}\right)P_m$	$\left(\frac{\partial \Phi_{cp}}{\partial S_p}\right)P_{S_p}$	$P_{\Phi_{cp}}$
			cal/deg mole			
0.090964	0.00004	-41.5	4.5	0.16	5.47	5.5
0.16061	0.00007	-35.1	-0.2	0.15	3.09	3.1
0.24919	0.00012	-28.7	-1.2	0.16	1.99	2.0
0.35767	0.00018	-22.3	-0.2	0.16	1.39	1.4
0.48758	0.00025	-15.8	-0.2	0.15	1.02	1.0
0.64128	0.00034	-9.2	-0.2	0.15	0.77	0.8
0.80241	0.00045	-3.2	0.4	0.15	0.62	0.6
0.98030	0.00057	2.6	0.3	0.15	0.51	0.5
1.2070	0.0008	9.2	-0.2	0.15	0.42	0.4
1.4501	0.0010	15.3	0.1	0.15	0.35	0.4
1.7012	0.0012	20.8	0.1	0.14	0.30	0.3
1.9675	0.0014	26.0	0.0	0.13	0.27	0.3
2.2577	0.0018	30.9	-0.2	0.14	0.24	0.3
2.5693	0.0021	35.6	0.1	0.13	0.21	0.2
2.8997	0.0025	39.9	0.1	0.13	0.19	0.2
3.2554	0.0030	43.9	0.0	0.13	0.18	0.2
3.6100	0.0035	47.2	-0.1	0.13	0.16	0.2
3.8771	0.0038	49.0	0.0	0.12	0.15	0.2
4.2800	0.0043	52.3	0.0	0.12	0.14	0.2
		Average	0.4		Average	0.9

[a] Φ_{cp} calculated from L.S. fit.

[b] $\Delta = \Phi_{cp}{}^a - \Phi_{cp}$ (experimental).

Table 27. Probable error in molality and in the apparent molal heat capacity for $Sm(ClO_4)_3$ solutions

m	P_m	$\Phi_{cp}{}^a$	Δ^b	$\left(\frac{\partial \Phi_{cp}}{\partial m}\right)P_m$	$\left(\frac{\partial \Phi_{cp}}{\partial S_p}\right)P_{S_p}$	$P_{\Phi_{cp}}$
			cal/deg mole			
0.092050	0.00003	-25.2	1.8	0.15	5.41	5.4
0.16020	0.00006	-19.3	0.6	0.16	3.11	3.1
0.24913	0.00008	-13.6	0.4	0.13	2.00	2.0
0.35881	0.00015	-8.4	0.6	0.16	1.39	1.4
0.48671	0.00020	-3.6	0.0	0.15	1.02	1.0
0.63895	0.00027	1.0	0.1	0.15	0.78	0.8
0.80385	0.00037	5.2	-0.3	0.15	0.62	0.6
0.99739	0.00049	9.2	-0.3	0.15	0.51	0.5
1.2095	0.0006	13.2	-0.3	0.14	0.42	0.4
1.4388	0.0008	16.7	-0.1	0.15	0.36	0.4
1.6828	0.0010	20.2	0.0	0.14	0.31	0.3
1.9487	0.0013	23.6	0.1	0.15	0.27	0.3
2.2445	0.0015	27.2	0.2	0.14	0.24	0.3
2.5482	0.0018	30.7	0.4	0.14	0.21	0.3
2.8832	0.0023	34.4	0.1	0.14	0.19	0.2
3.2291	0.0027	38.2	-0.2	0.14	0.17	0.2
3.5951	0.0032	42.1	-0.3	0.14	0.16	0.2
3.9753	0.0038	46.3	0.0	0.14	0.15	0.2
4.3237	0.0043	50.1	-0.1	0.13	0.14	0.2
4.6400	0.0046	53.7	0.3	0.13	0.13	0.2
		Average	0.3		Average	0.9

[a] Φ_{cp} calculated from L.S. fit.

[b] $\Delta = \Phi_{cp}{}^a - \Phi_{cp}$ (experimental).

from the values listed under the heading $(\partial\Phi_{cp}/\partial m)_{S_p} P_m$ in Tables 26 and 27 with the constant being about 0.15 cal/deg mole. This in effect would shift the whole Φ_{cp} versus $m^{1/2}$ curve 0.15 cal/deg mole up or down depending on the sign of the error in m.

In order to calculate $\overline{C}_{p1}$ and $\overline{C}_{p2}$, Φ_{cp} data was expressed as an analytic function of concentration using a least squares method. The function chosen was a polynomial expanded in orders of $m^{1/2}$ because Φ_{cp} approximates a linear function versus $m^{1/2}$. $\overline{C}_{p1}$ and $\overline{C}_{p2}$ as calculated from Equation 2.15 and 2.14 are dependent on the derivative of Φ_{cp} with respect to $m^{1/2}$ and therefore are sensitive functions of the coefficients of the polynomial used. Because it is not known if the polynomial used is the best possible function that should be employed to express Φ_{cp} versus concentration, there is no way of quantitatively determining errors in $\overline{C}_{p1}$ and $\overline{C}_{p2}$.

Qualitatively, it is known by comparing fits of data with different degree polynomials that the derivatives of the polynomials become more uncertain at the borders of the data set. Therefore, values for $\overline{C}_{p1}$ and $\overline{C}_{p2}$ are more uncertain for the most concentrated solutions than for solutions in the middle of the concentration range. At the lower end of the data set where the solutions are dilute, $\overline{C}_{p1}$ must approach the value for the heat capacity of pure water, and values for $\overline{C}_{p1}$ in this concentration region become more accurate. The

values for $\overline{C}_{p2}$ in the dilute region become more uncertain with decreasing concentration because in addition to the uncertainty of the derivative of Φ_{cp} with respect to $m^{1/2}$ near the border of the data set, the probable error in the value for Φ_{cp} increases.

The average deviation of the polynomial fits for both $Sm(NO_3)_3$ and $Sm(ClO_4)_3$ is less than that predicated from the probable errors of Φ_{cp}. It is not felt that the data was over fitted, but that the 0.05% of S_p taken as the probable error for the specific heat capacity was too high since this is the maximum error expected. Additionally, an error in the molality of the stock solution would not cause any scatter of the data because this error is prorated over all the solutions prepared from the stock solution.

V. DISCUSSION

A. Heat Capacity of Pure Water and of Solutions

Pure liquid water is a very complex substance, and although its properties have been thoroughly studied, the interpretation of these properties with regard to microscopic behavior has not been settled. At present, researchers in this area are divided into two camps. Both sides believe that liquid water is highly associated due to hydrogen-bonding, but one side believes that a hydrogen-bond can be bent and therefore has a continuous range of energies; the other side believes that hydrogen-bonds have only one energy and are either broken or unbroken with partial bond character not allowed.

Models for liquid water utilizing these two different concepts have been formulated. Because calculations of the macroscopic properties of water from these models involve the use of approximations and parameters, it is usually possible that two different models can both predict the correct values for the macroscopic property in question. Therefore, it is not possible at this time to discern which is the correct concept of the hydrogen-bonded structure of water. A book written recently by Eisenberg and Kauzmann (35) provides an excellent review of the properties of H_2O in all of its phases and of the use of these properties in the interpretation of possible microscopic behavior. For the sake

of simplicity the following discussion will consider that hydrogen-bonds in water are either broken or unbroken, although the concept of bent hydrogen-bonds could also be used in explaining the heat capacity of water.

Pure liquid water with its nine degrees of freedom, of which three (vibrational) are essentially not excited, has a large heat capacity of 18 cal/deg mole. Part of this large heat capacity has been ascribed to the fact that water, because of hydrogen-bonding, is a highly structured liquid. When the temperature of water is raised, hydrogen-bonds are broken and some of the structure is destroyed. This results in a contribution to the heat capacity given by

$$C_z = \Delta H \frac{dz}{dT}$$

where ΔH is the enthalpy of formation of a hydrogen-bond, z is the number of hydrogen-bonds per mole of water, and T is temperature.

It is also believed that addition of highly charged electrolytes to water causes a decrease in the structure of water, i.e., z decreases. This decrease in the number of hydrogen-bonds should cause a corresponding decrease in the heat capacity of water since the contribution C_z would be less if there were fewer hydrogen-bonds left to break.

The difference between the value of the heat capacity of a dilute aqueous solution of highly charged ions and

the value for the heat capacity of the water alone can then be considered the result of opposing contributions, i.e., a positive contribution due to the intrinsic heat capacity of the ions plus the heat capacity of the ion hydrates formed, and a negative contribution due to the decrease in heat capacity associated with a decrease in hydrogen-bonding of the water that enters the ions' spheres of influence. This is, of course, an over-simplification and as is pointed out by Holtzer and Emerson (36) arguments based on the concept of the structure of water should be considered with some reservation. However, even though the behavior in solution is complex, using this simple idea is instructive in understanding part of what is occurring in aqueous solutions of electrolytes.

As can be seen in Figures 4 through 7, the addition of a small amount of rare earth salt to 1,000 gm of water causes an initial decrease in the heat capacity of the water. This is understandable because the trivalent rare earth ions with their high charge densities hydrate strongly resulting in the negative contribution to the heat capacity being greater than the positive contribution. $\overline{C}_{p2}$ and Φ_{cp}, previously defined by Equations 2.9 and 2.8, respectively, are therefore both negative for dilute solutions as also shown in Figures 4 through 7.

As more salt is added to the solution resulting in higher concentrations, the contribution of the intrinsic heat capacity

of the ions plus the heat capacity of the ion hydrates begins to predominate over the negative contribution. This occurs because the negative contribution decreases with increasing concentration as there are fewer hydrogen-bonds left in solution to be destroyed with an increase in temperature. A concentration is reached where the positive and negative contributions resulting from the addition of a small amount of salt are equal, and the heat capacity of the solution does not change with the addition of salt, i.e., $dC_p/dn_2 = 0$ as is evidenced by the minima in the heat capacity of 1,000 gm H_2O plus m moles of rare earth salt versus molality curves of Figures 4 through 7. $\overline{C}_{p2}$ is therefore zero at this point and is positive at higher concentrations since $dC_p/dn_2 > 0$ as is seen in Figures 4 through 7.

As $\overline{C}_{p2}$ values increase with concentration, the corresponding values for $\overline{C}_{p1}$ decrease as required by Equation 2.16.

$$\frac{d\overline{C}_{p1}}{dm} = -\frac{mM_1}{1,000}\frac{d\overline{C}_{p2}}{dm} \tag{2.16}$$

Physically this can be understood by considering that in dilute solutions the heat capacity of the water decreases with increasing ion-water interactions, and that ion-water interactions increase with concentration. The curves of $\overline{C}_{p1}$ versus molality are shown in Figures 4 through 7.

At high concentrations where occurrences such as complexing between cation and anion may become prevalent, unusual behavior of $\bar{C}_{p1}$ and $\bar{C}_{p2}$ may be observed. For instance, an anion entering the first hydration shell of the rare earth ion and forming an inter-sphere complex would replace water and allow it to return to the bulk phase. Also, formation of inner-sphere complexes would convert the +3 rare earth ions involved in complexation to species with lower charge thus decreasing the ionic strength of the solution. Both of these effects would cause the heat capacity of the water in solution to increase. Thus, with increasing concentration $d\bar{C}_{p1}/dm$ would become less negative with a corresponding decrease in $d\bar{C}_{p2}/dm$. This idea in relation to $\bar{C}_{p1}$ and $\bar{C}_{p2}$ versus molality for the rare earth perchlorates and nitrates will be discussed further under their respective headings.

The heat capacities of the solutions were measured at constant pressure for practical reasons. However, heat capacities at constant volume, C_v, are of more interest because no work term is involved. C_v can be calculated from C_p and the equation of state for the solution in question, but for rare earth perchlorate and nitrate solutions the temperature and pressure dependence of the volume is not known, and the calculation cannot be made at this time.

The regular decrease of the radii of the chemically similar trivalent rare earth ions going from La^{3+}, 1.061Å,

to Lu^{+3}, 0.848Å (8), provides a means of studying a series of salt solutions to determine the effect of ionic radius on solution properties. It might be expected that, like the ionic radius, the solution properties of the rare earth salts would vary regularly across the series. This has not been found to be the case.

B. Perchlorates

As observed from Figure 8 the apparent molal heat capacities, Φ_{cp}, for the rare earth perchlorate solutions do not follow a regular trend across the rare earth series. It might be expected that Φ_{cp} would decrease across the rare earth series with decreasing ionic radii of the rare earth ions using the theory the smaller the ion, the higher its charge density and the greater its influence on the water around it. This should mean more water molecules are affected and result in a smaller value for Φ_{cp}.

What is observed in Figure 8 for the two dilute solutions at 0.4 and 1.0 molal is level or slightly decreasing behavior of Φ_{cp} versus rare earth for the rare earths La to Nd and Ho to Lu with Φ_{cp} increasing for the rare earths between Nd and Ho. A similar trend across the rare earth series has been observed in other properties such as apparent molal volumes, Φ_V, (9,10,11) and relative apparent molal heat contents, Φ_L, (12,13,21). The behavior of Φ_V's and Φ_L's has been explained in terms of two series within the rare earths. The first

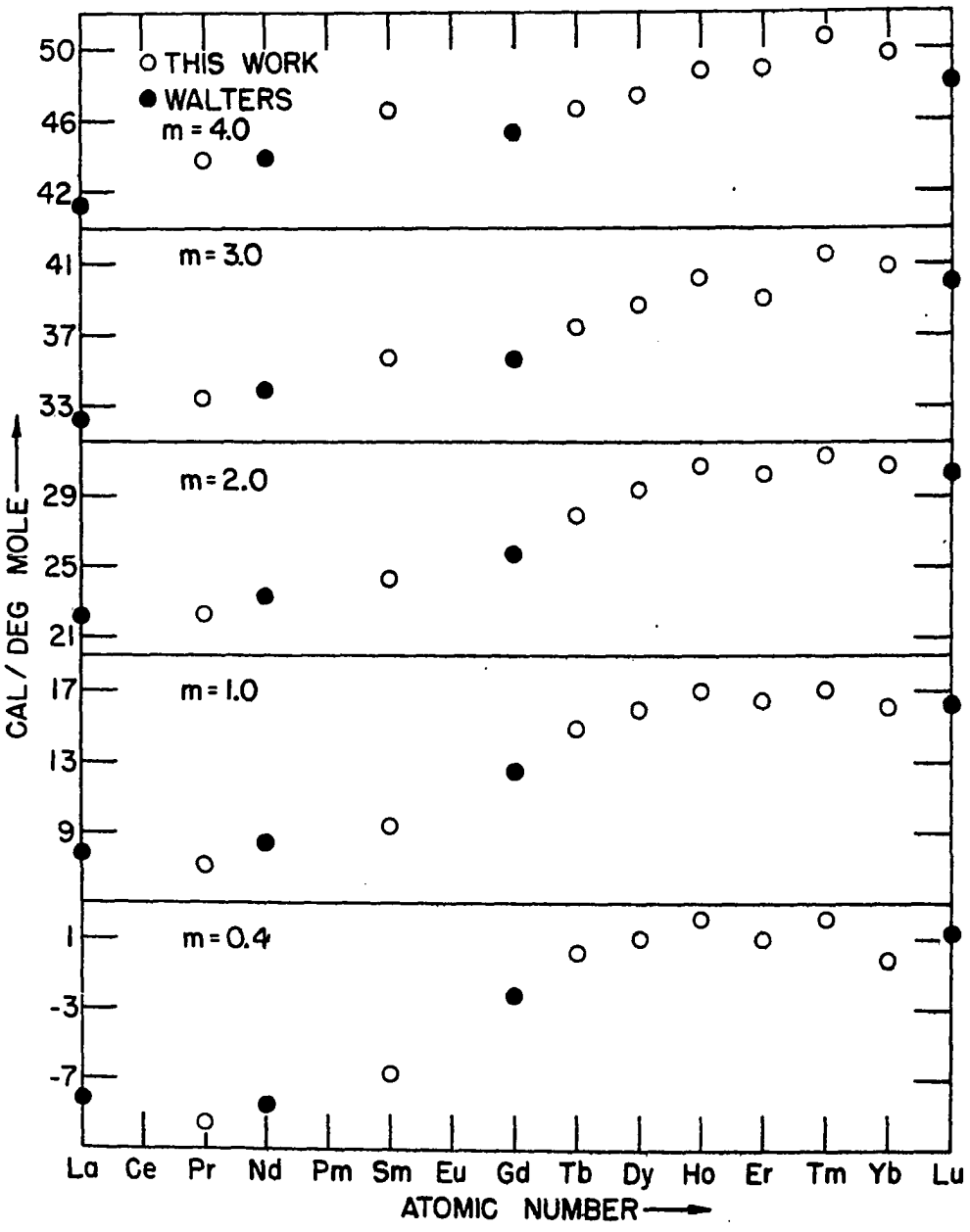

Figure 8. Apparent molal heat capacity of aqueous $RE(ClO_4)_3$ solutions at various molalities and 25°C

series includes the larger ions La to Nd which are considered to have a constant coordination number in dilute solutions. The other series includes the smaller ions Tb to Lu which are also considered to have a constant coordination number, but this number is considered to be one less than the coordination number for the light rare earths. Furthermore, the ions between Nd and Tb are considered to exist in solution as an equilibrium of the two coordination types with the equilibrium shifting rapidly with decreasing ionic radius from the higher to the lower coordination type.

Other researchers have also explained their data (37,38) by considering that the intermediate rare earth ions exist in solution as an equilibrium of two hydrated species with different coordination numbers. There is ample additional evidence from solid rare earth compounds that a decrease in the coordination number of the rare earth ion occurs with increasing atomic number (39,40,41,42,43). Work on crystal structures shows that coordination numbers for the rare earths can range from 6 up to possibly 12 with the number generally greater than 6 (40).

Pikal (10,44) using geometrical models for hydrated rare earth ions in solution was able to show that a coordination number of 9 for the rare earth ions La^{3+} to Nd^{3+} and 8 for Tb^{3+} to Lu^{3+} were compatible with Φ_V data extrapolated to infinite dilution. The rare earth ions Sm^{3+}, Eu^{3+}, and Gd^{3+}

were assumed to exist in solution as equilibrium mixtures of the hydrated species $RE(H_2O)_9^{3+}$ and $RE(H_2O)_8^{3+}$.

The trend of Φ_{cp} across the rare earth series can also be explained in terms of two series within the rare earths with different coordination numbers. In dilute solutions the light rare earths La to Nd which form one series have values for Φ_{cp} which are less than the values for Φ_{cp} of the other series composed of the heavy rare earths Ho to Lu. This would be expected if, as supposed, the coordination number for the heavy series is less than that for the light since Φ_{cp} should be greater for the rare earths affecting the fewer water molecules. Likewise, it would be expected that Φ_{cp} would increase with decreasing atomic radius for the rare earths between Nd and Ho since it is believed that these ions exist in solution as an equilibrium of the two coordination types with the equilibrium shifting rapidly from the higher to the lower coordination with decreasing ionic radius. Whether or not the coordination numbers are 9 and 8 as suggested by Pikal cannot be determined from this work.

The difference between Φ_{cp} for Gd in the higher coordination type obtained by extrapolation from the light rare earth series and Φ_{cp} for Gd in the lower coordination type obtained by extrapolation from the heavy rare earth series is roughly 13 cal/deg mole at m = 0.4. This is a reasonable

value for the supposition that the difference in coordination numbers is one since the heat capacity of pure water is 18 cal/deg mole. The difference in the extrapolated values of Φ_{cp} for Gd in the two coordination types decreases to about 10 cal/deg mole for solutions at one molal and for solutions at two and three molal, Φ_{cp} is generally increasing with increasing atomic number for all the rare earths up to Ho. This may imply that at higher concentrations even the light rare earths exhibit some tendency to form hydrates with the lower coordination number, and that the equilibrium shifts toward the lower coordination with increasing concentration for both the light and intermediate rare earths. As further evidence for the tendency of the light rare earth ions to exist in solution as an equilibrium between two coordination types, Nakamura and Kawamura (45) have explained their nuclear magnetic relaxation data of the perchlorate and chloride solutions of $^{139}La^{3+}$ in terms of the existence of an equilibrium between two hydrated species such as $La(H_2O)_8^{3+}$ and $La(H_2O)_9^{3+}$.

In dilute solutions it might be expected that ions affecting the structure of water the least would have the largest values for $\overline{C}_{pl}$. The trend in $\overline{C}_{pl}$ versus rare earth for rare earth perchlorate solutions is shown in Figure 9. The increase around Sm and Gd is then interpreted as further evidence for a coordination change occurring across the rare earth series with the light rare earths existing in solution

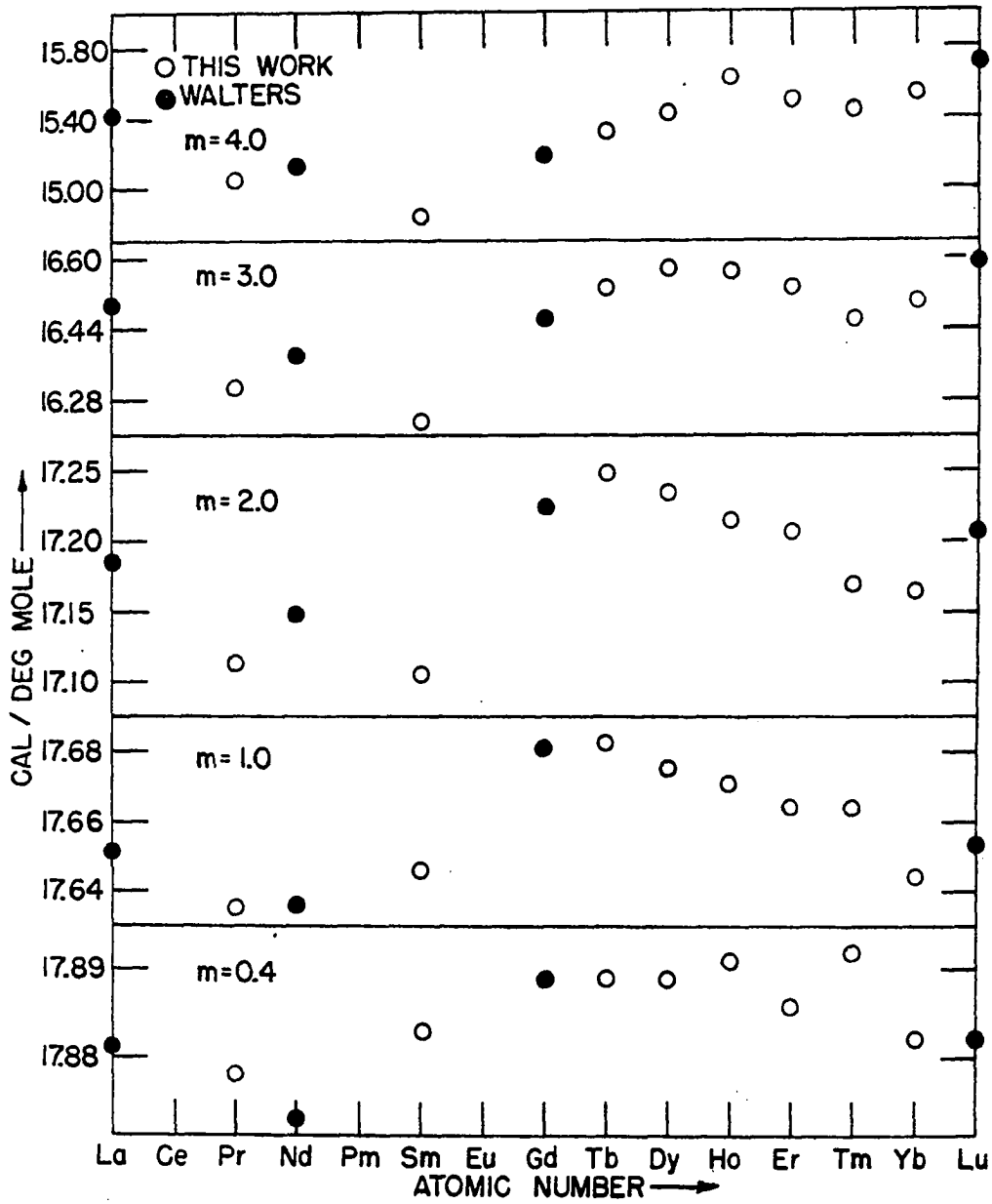

Figure 9. Partial molal heat capacity of the solvent for aqueous $RE(ClO_4)_3$ solutions at various molalities and 25°C

with a larger first sphere coordination number than the heavy rare earths.

As is apparent from Figures 4 through 7, $\overline{C}_{p1}$ and $\overline{C}_{p2}$ for the rare earth perchlorates exhibit no unusual behavior such as an upturn in $\overline{C}_{p1}$ and a corresponding downturn in $\overline{C}_{p2}$ at any concentration. This implies, as has often been assumed, that the perchlorate ion does not form inner-sphere complexes with the trivalent rare earth ions.

Further evidence against inner-sphere coordination of metal ions by perchlorate ions in solution has been presented by Hester and Plane. The free perchlorate anion which has T_d point group symmetry would be expected to have a lower symmetry such as C_{3v} if it coordinated with a metal ion. The lowering of symmetry with coordination would result in the removal of some of the degeneracies of the degenerate vibrational modes associated with T_d symmetry. Hester and Plane in their Raman studies of aqueous solutions (46) observed only four vibrational bands for the perchlorate anion in La^{3+} solutions as predicted by T_d symmetry as opposed to six predicted for C_{3v} symmetry. Likewise, in this laboratory[1] only four vibrational bands were observed for the perchlorate anion in other rare earth perchlorate solutions over all concentration ranges.

---

[1]Spedding, F. H., M. A. Brown and B. Mundy, Ames, Iowa, Private communication, 1971.

At the highest concentrations behavior in solution becomes even more complex because the amount of water present may be less than that necessary to form the normal hydrates of the cations and anions. This may force the cations and anions to share water molecules resulting in the formation of outer-sphere complexes. It has been suggested (47,48) that perchlorate ions do form outer-sphere complexes with various metals in concentrated solutions. Although no evidence for the formation of outer-sphere complexes was found, it is not known how sensitive heat capacities are to formation of such complexes.

C. Nitrates

The trend of apparent molal volumes, Φ_V, across the rare earth series have provided evidence for the theory that in infinitely dilute nitrate solutions (9,11) the light rare earths have one coordination number, the heavy rare earths have a different coordination that is smaller, and the intermediate rare earths such as Sm, Eu, and Gd exist as equilibrium mixtures of species with these two different coordination numbers. However, at finite rare earth nitrate concentrations of a few thousandths molal this evidence starts to become obscured. This has been explained by Cullen (11) and Ayers (9) as the result of the formation of rare earth complexes with the nitrate anion. It is understandable then that Φ_{cp} data for the rare earth nitrate solutions shown in Figure 10

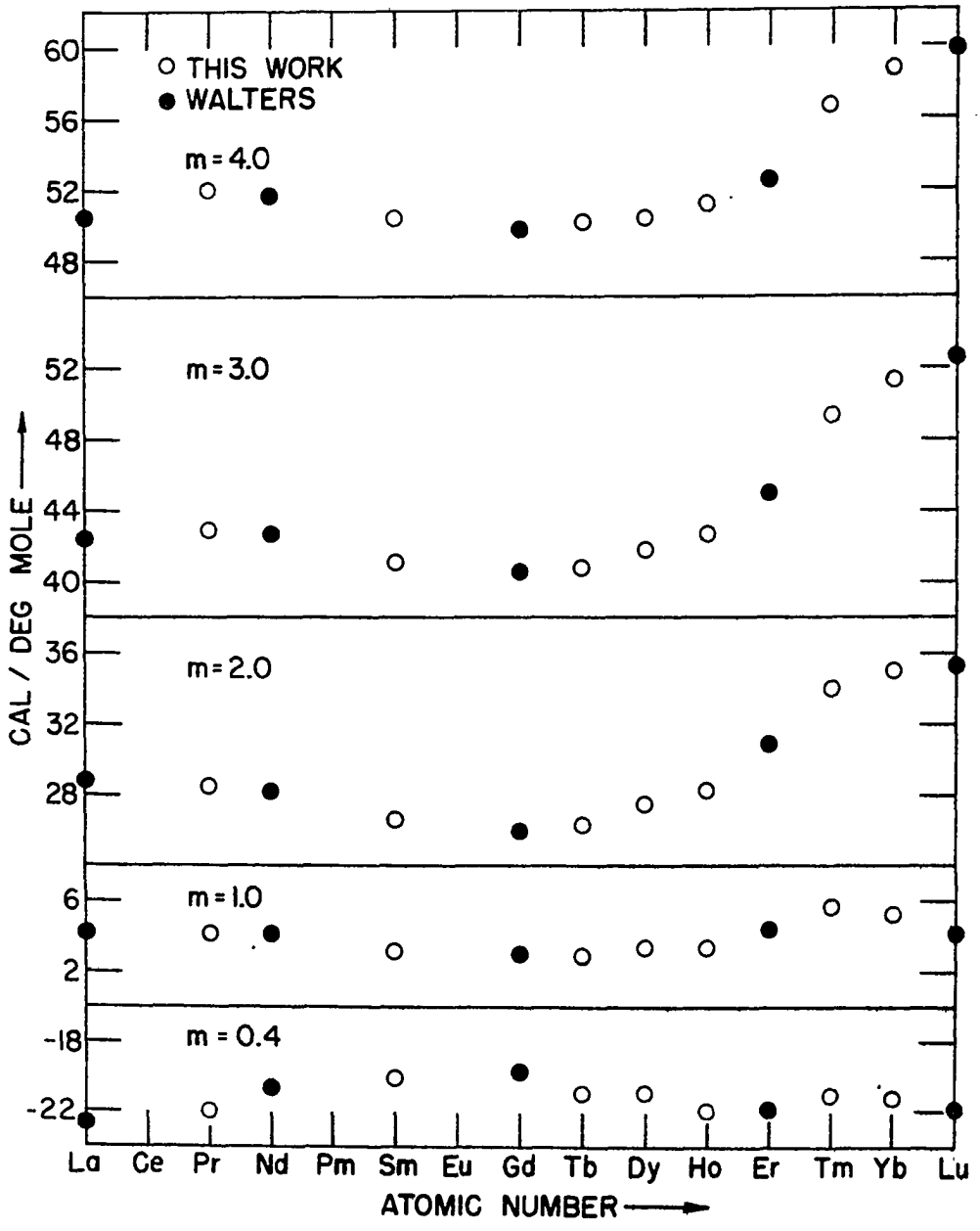

Figure 10. Apparent molal heat capacity of aqueous $RE(NO_3)_3$ solutions at various molalities and 25°C

do not show the behavior associated with a coordination change as the Φ_{cp} data were taken at concentrations much greater than a few thousandths molal.

The deviation in the behavior of Φ_v versus molality as noted by Cullen (11) was greatest for the light rare earths La to Gd. Corresponding to this, the values for the first stability constants defined by

$$K_c = \frac{[RENO_3^{2+}]}{[RE^{3+}]\,[NO_3^-]} \qquad (5.1)$$

as determined by Peppard, et al. (49) at an ionic strength of 1μ are greatest for the light rare earths increasing from 1.3 liter/mole for La to 2.0 liter/mole for Eu and then dropping off for the heavy rare earths beyond Gd where Tm has a value for K_c of 0.7 liter/mole. As expressed by Abrahamer and Marcus (50), the governing factor for complex formation is the competition of the complexing ligands with the hydrating water ligands. Working with organic solvents, they determined that water and the nitrate ion have about the same affinity for rare earth ions. However, the free energy changes involving the transfer of ligands, either water or nitrate ions, from the bulk solvent phase to the vicinity of the rare earth ion is probably considerably different in aqueous solutions due to the highly structured nature of liquid water.

It is established that the nitrate ion does complex with rare earth ions but there is discussion as to whether complexing is inner-sphere or outer-sphere. Choppin and Strazik (51) from thermodynamic data for the formation of $EuNO_3^{2+}$ propose, using the model of Frank and Evans (52) for electrolyte solutions, that $EuNO_3^{2+}$ is an outer-sphere complex. More recently Bukietynska and Choppin have published spectroscopic data (53) involving f → f transitions which they feel indicate the formation of $NdNO_3^{2+}$ inner-sphere complexes to a limited extent.

There is, on the other hand, a large amount of evidence that the nitrate ion forms predominately the inner-sphere complex with rare earth ions with possibly some outer-sphere complexing taking place. Reuben and Fiat found in their nuclear magnetic resonance studies (54) that the position of the ^{17}O resonance of ^{17}O enriched water is shifted upon addition of paramagnetic Dy^{3+} ions [added as $Dy(ClO_4)_3$] and that this shift is linear with Dy^{3+} concentration. They also found that the addition of nitrate (added as $LiNO_3$) to a 0.473 molal solution of $Dy(ClO_4)_3$ in ^{17}O enriched water caused the shift to decrease. The decrease in the shift was interpreted in terms of a decrease in the number of water molecules in the first coordination sphere of the Dy^{3+} ion resulting from the replacement of water by nitrate ions forming inner-sphere complexes. As evidence that the nitrate ions are indeed entering the first coordination sphere of Dy^{3+} ions, they

observed that the ^{17}O resonance of ^{17}O labeled nitrate in $LiN^{17}O_3$ solutions is shifted upon the addition of paramagnetic Dy^{3+} ions.

The free nitrate ion in solution has D_{3h} symmetry resulting in three Raman active vibrational modes of which two are doubly degenerate. Should a nitrate ion coordinate with a rare earth ion, through either one or two oxygen atoms, the D_{3h} symmetry of the nitrate ion would be reduced to C_{2v} symmetry resulting in the removal of the degeneracy of the two degenerate modes.

Hester and Plane (46) have found that in concentrated $Ce(NO_3)_3$ solutions the Raman bands for the vibrational modes of the nitrate ion are split implying some of the nitrate ions exist with C_{2v} symmetry, and they conclude that the extreme distortion of the nitrate symmetry makes it highly probable that the complexing is the inner-sphere type. Likewise, Raman data from this laboratory[1] also show distortion of the nitrate symmetry for a number of rare earth nitrates again implying inner-sphere complexing.

Knoeck (55) working with the infrared spectra of $La(NO_3)_3$ solutions reported the appearance of a vibration band for the nitrate ion that is infrared forbidden by D_{3h} symmetry but permitted by C_{2v} symmetry. Additionally, he reported the removal

---

[1]Spedding, F. H., M. A. Brown and B. Mundy, Ames, Iowa, Private communication, 1971.

of the degeneracy for the degenerate vibrational modes from which he concluded that the nitrate ion was forming inner-sphere complexes with La^{3+}.

From a study of the nuclear magnetic relaxation of ^{139}La solutions with nitrate ions present, Nakamura and Kawamura (45) use inner-sphere $LaNO_3^{2+}$ complexes to explain the variation of relaxation times with nitrate concentration. Abrahamer and Marcus (56) using density, NMR, and molar absorptivity studies on $Er(NO_3)_3$ concluded that Er^{3+} formed mainly inner-sphere complexes with nitrate ions with some outer-sphere complexing occurring.

The data from this work are in agreement with the contention that the nitrate ions form inner-sphere complexes with the rare earth ions. As is apparent from Figures 4 through 7, at high concentrations $d\bar{C}_{pl}/dm$ becomes less negative and ultimately becomes positive. This is true for all the rare earths except La where $d\bar{C}_{pl}/dm$ also becomes less negative at high concentrations but the solution becomes saturated before $d\bar{C}_{pl}/dm$ can become positive. This behavior of $d\bar{C}_{pl}/dm$ for the rare earth nitrates implies that nitrate ions are entering the first hydration sphere and releasing water to the bulk phase. In the case of $Tm(NO_3)_3$, $Yb(NO_3)_3$, and $Lu(NO_3)_3$ the upturn is so great that the values of $\bar{C}_{pl}$ for concentrated solutions approach the value for the heat capacity of pure water. It may be in these solutions that most if not all of the rare earth exists as a neutral

trinitrate species. Conductance measurements to be made in this laboratory should confirm or deny this idea.

There is also the question of whether the nitrate ion, if it forms inner-sphere complexes with the rare earth ions in solution, is monodentate or bidentate in its coordination to the rare earth ion. Knoeck (55) from his infrared work stated that the depolarization ratio of the 1,400 cm^{-1} spectral envelope is indicative of bidentate nitrate coordination to the La^{3+} ion. Reuben and Fiat (54) in their NMR work concluded that each nitrate ion entering the inner-sphere of the Dy^{3+} ion replaced two water molecules and acted as a bidentate ligand. Although it is at best only an approximation to compare behavior in the solid state with solution behavior, Rumanova, et al. (57) have reported three nitrate ions and four water molecules in the first coordination sphere of praseodymium from their structural study of $Pr(NO_3)_3 \cdot 6H_2O$ with two oxygens of each nitrate adjacent to the praseodymium.

Recently Nelson and Irish (58) have made a Raman and infrared study of aqueous gadolinium nitrate solutions over a wide range of compositions. They believe their detailed intensity analyses of the nitrate ions' vibrational spectra indicate that the predominant species in solutions with nitrate to gadolinium ratios less than two is $Gd(NO_3)_2^+$ with one nitrate ion binding through two oxygen atoms and

the other through one. Furthermore, they present possible evidence for a bridging, polynuclear aggregate of cations and anions in systems of low water content.

The data from this work expecially for the heavy rare earth nitrates indicate that upon complexing each nitrate ion replaces more than one water molecule since the values for $\bar{C}_{pl}$ at higher concentrations as listed in Table 21 become quite large. However, in light of all the possible types of coordination, to conclude bidentate nitrate coordination from this data would be speculation.

There is little data in the literature for stability constants of the rare earth nitrates determined as a function of ionic strength. Most of the data available is listed in Table 28 at ionic strengths of 1μ and 4 to 4.2μ.

It is apparent from Table 28 that for dilute solutions (an ionic strength of 1μ corresponds to a 0.1667 molal rare earth solution) the light rare earths complex with the nitrate ion more than the heavy rare earths. In slightly more concentrated solutions (4μ corresponds to a 0.6667 molal rare earth solution) it appears that the light rare earths are still complexing more than the heavy rare earths, but that the difference in the amount of complexing between the light and heavy rare earths has decreased. It should be noted that even though K_c has decreased with increasing ionic strength, the percentage of rare earth ions that form complexes

Table 28. Stability constants (K_c) of $RE(NO_3)_3$ solutions

Salt	K_c at 1μ	Salt	K_c at 4 to 4.2μ
$La(NO_3)_3$[a]	1.3	$Pr(NO_3)_3$[b]	0.66
$Ce(NO_3)_3$[a]	1.3	$Nd(NO_3)_3$[c]	0.77
$Pr(NO_3)_3$[a]	1.7	$Sm(NO_3)_3$[b]	0.95
$Eu(NO_3)_3$[a]	2.0	$Er(NO_3)_3$[b]	0.54
$Tm(NO_3)_3$[a]	0.7		
$Yb(NO_3)_3$[a]	0.6		
$Lu(NO_3)_3$[a]	0.6		

[a]Work done by Peppard, et al. (49).

[b]Work done by Anagnostopoulos and Sakellaridis (59).

[c]Work done by Coward and Kiser (60).

with the nitrate ions has increased because of the increased concentrations of the reactants and the mass action principle.

Values for $\bar{C}_{pl}$ versus rare earth as observed in Figure 11 for dilute solutions (0.4 and 1.0 molal) can be correlated with the trend in stability constants of the rare earth nitrates as both $\bar{C}_{pl}$ and K_c values increase to a maximum in the middle of the rare earth series and then decrease. This correlation is expected because values for $\bar{C}_{pl}$ should be largest for solutions where the amount of complexing is the greatest since a nitrate ion entering the first coordination

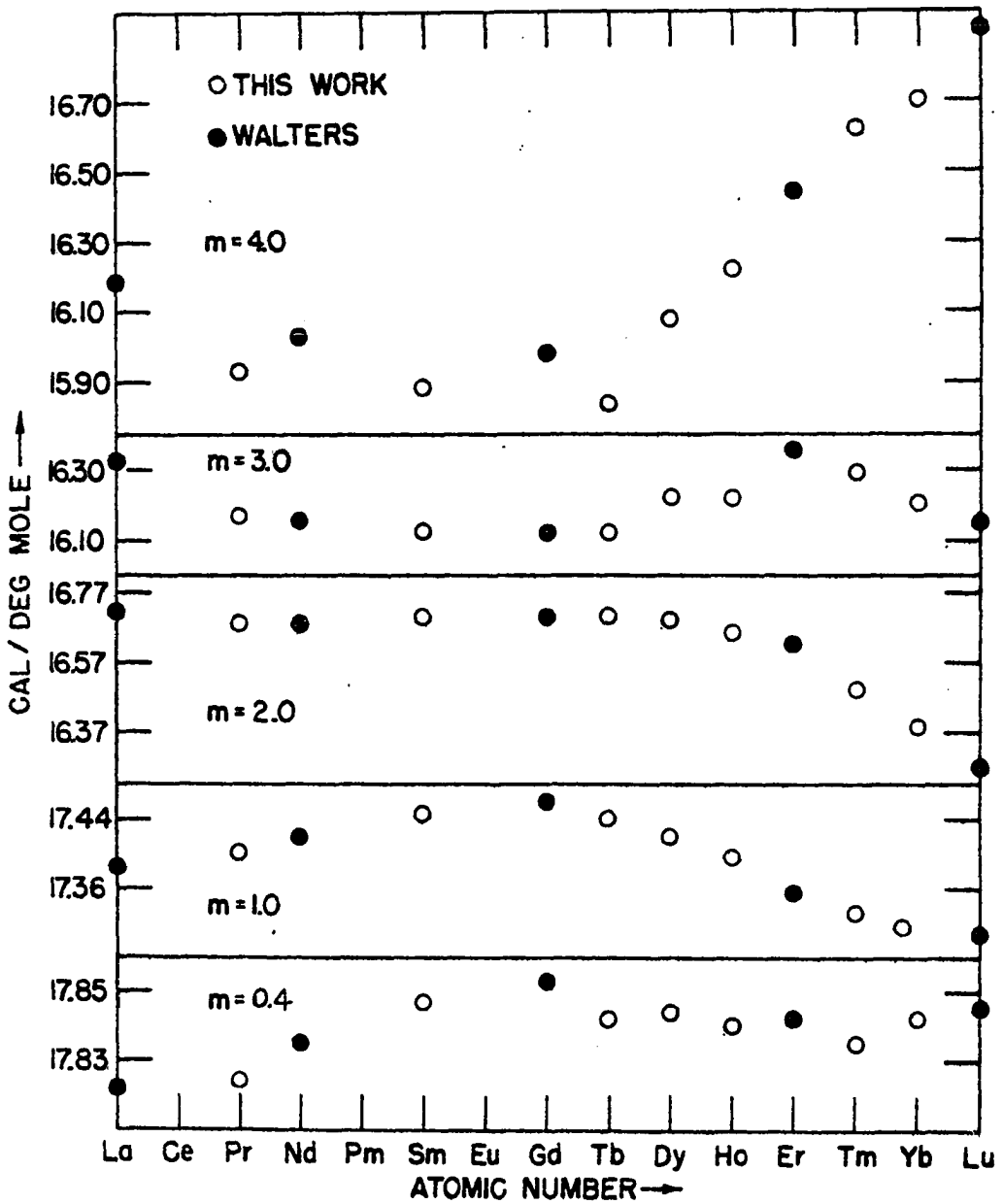

Figure 11. Partial molal heat capacity of the solvent for aqueous $RE(NO_3)_3$ solutions at various molalities and 25°C

sphere would replace water and also reduce the ionic strength of the solution. Both of these effects should result in a higher heat capacity for the water in solution.

At higher concentrations (greater than one molal) the first stability constants of the light rare earths may decrease to values less than those for the heavy rare earths; in addition, the second and third stability constants for the formation of the dinitrate and trinitrate complexes become important in determining the amount of complexing. The result may be that at higher concentrations the average number of nitrate ions coordinated to a rare earth ion may be greater for the heavy rare earths than for the light. Evidence for this supposition is observed in Figure 11 where at a concentration of 3.0 molal values for $\overline{C}_{pl}$ for the heavy rare earths are becoming larger than those for the light rare earths and at 4.0 molal the heavy rare earths exhibit increasing values of $\overline{C}_{pl}$ with increasing atomic number.

Additional possible evidence for the idea that in concentrated solutions the heavy rare earths complex more than the light rare earths is noted in work by Peppard, et al. (61). In studies of liquid extraction of rare earth nitrates from an aqueous HNO_3 phase into TBP (tributylphosphate) it was found that above eight molar HNO_3 the extractability of the rare earths increased with atomic number paralleling the theoretical order of decreasing basicity. However, Peppard,

et al. (61,62) noted that at certain acid concentrations below 8 molar, e.g., 2.94 molar, that the order of extractability was inverted with the light rare earths being more extractable than the heavy rare earths. It is proposed that the species extracted is $RE(NO_3)_3 \cdot 3$ TBP so it is reasonable to believe that the rare earth that complexed the most in the aqueous phase would be more extractable into the organic phase.

Karraker (39), in assessing Peppard's data, suggests the inversion in extractability is due to a change in the coordination number of the species $RE(NO_3)_3 \cdot 3$ TBP with the three nitrates being coordinated in a monodentate manner for the heavy rare earths and two of three coordinated in a bidentate manner for the light rare earths. Some Russian workers (63) however believe the extracted species is $RE(NO_3)_3 \cdot 3\ HNO_3$. It is evident then that liquid extraction is a complex phenomenon involving many variables which are not completely understood, and conclusions drawn from the magnitude and order of distribution constants must be considered with some reservation.

D. Chlorides

The data on the rare earth chloride solutions collected in this laboratory by Jones and Walters have been discussed elsewhere (14,15,16). They saw evidence in dilute solutions for a change occurring in the coordination of water molecules

about the intermediate rare earth ions, with the heavy rare earth ions having a smaller coordination number than the light rare earth ions. They also saw behavior in concentrated solutions indicative of cation-anion interactions such as complexing of the rare earth ion by the chloride ion. For the sake of comparison, the data on rare earth chloride solutions were included with that on the rare earth nitrates and perchlorates illustrated in Figures 4 through 7.

E. Comparison of Salts with Different Anions

From Figures 4 through 7 it is apparent that in dilute solutions the heat capacities for a given rare earth are in the order ClO_4^- > NO_3^- > Cl^-. This order is also the same for the heat capacities of dilute solutions of the sodium salts of these anions (32,33,64). From a calculation of the vibrational heat capacity assuming harmonic oscillators and using the frequencies and assignments for the vibrational modes of the ClO_4^- and NO_3^- ions given by Herzberg (65), it was determined that C_{vib} = 6.7 cal/deg mole anion for ClO_4^- and 2.7 cal/deg mole anion for NO_3^-. Of course, Cl^- has no internal vibrational degrees of freedom and, hence, no vibrational heat capacity. The order of ClO_4^- > NO_3^- > Cl^- as observed is the same as the order of vibrational heat capacities for the anions.

The vibrational heat capacities of anions alone do not explain the order in the heat capacities however because

after subtracting out the difference (4.0 cal/deg mole anion) between the vibrational heat capacities of the ClO_4^- and NO_3^- ions, the heat capacities of $RE(ClO_4)_3$ solutions are still greater than $RE(NO_3)_3$ solutions up to about 1 molal. In dilute solution the other factors involved in determining the difference of the heat capacities are the interactions of the anions with the water; ion-ion interactions also become important as the concentration is increased. The effects on the heat capacity caused by anion-water interactions involve the effect of the anions on the structure of water including changing the potential barriers existing in pure water that restrict free rotation and translation of water molecules. Likewise, because of the formation of hydrates there is the effect of water restricting translation of the anions and in the case of ClO_4^- and NO_3^- restriction of rotation. Since the effects are many and varied, the result of these effects on the heat capacity of solutions cannot be calculated quantitatively at the present time. It should be possible to qualitatively explain the anion effect on heat capacity of solutions if more were known about anion-water and water-water interactions. Vibrational spectroscopy provides some information on these interactions.

The uncoupled O-D vibrational stretching band as observed in Raman and infrared spectra of dilute solutions of HDO in H_2O is slightly asymmetric and has a half-width of 160 cm^{-1}. The band maximum exhibits a small shift to higher frequencies

with increasing temperature. Since the band is quite wide (the same stretching band in ice I has a half-width of 30 cm^{-1}), it is generally believed that the band is an envelope of many narrow but overlapping bands associated with O-D oscillators in different environments. The same belief is held concerning the O-H oscillator in dilute solutions of HDO in D_2O where the half-width of the O-H stretching band is 270 cm^{-1} compared to 50 cm^{-1} in ice I.

Wall and Hornig (66) in 1965 used the idea of a continuous distribution of local environments in liquid water resulting in a continuous distribution of hydrogen-bond strengths to explain the bandshape and its temperature dependence. This idea corresponds to the distorted hydrogen-bond model for water. In more recent work on the temperature dependence of the O-D vibrational stretching band, it was observed from both Raman and infrared data that when the spectra at different temperatures were superimposed, the O-D stretching band could be resolved into at least two separate components or envelopes with a possible isobestic point between them. An isobestic point is a point of constant intensity, i.e., it is a common point through which all the spectra pass and is a phenomenon often associated with two absorbing species in equilibrium. The intensity of the high-frequency component increased and the intensity of the low-frequency component decreased with increasing temperature. These facts led the people who reported them, Walrafen (67) and Senior and Verrall (68), to

believe that the low-frequency component is associated with HDO molecules that are hydrogen-bonded, and that the high-frequency component is associated with HDO molecules that are not hydrogen-bonded. However, both components are quite broad, and the question has been raised (35) as to why the component assigned to the nonhydrogen-bonded HDO should be broad.

In addition to questions over the interpretation of vibrational spectrum of pure water, there is also controversy over the interpretation of the effects that added salt has on the vibrational spectrum of water. It is observed that the addition of alkali and alkaline earth perchlorate salts to dilute solutions of HDO in H_2O results in the splitting of the uncoupled O-D stretching band into two components (17,18,19,20). When the spectra of these solutions taken as a function of perchlorate concentration are superimposed they exhibit a possible isobestic point between components. This point occurs at very nearly the same frequency that it occurred at in the temperature dependence of the vibrational spectrum of pure water. Also, the intensity of the high-frequency component increases and the intensity of the low-frequency component decreases with increasing perchlorate concentration. Addition of perchlorate salts causes the same behavior to be observed for the O-H stretching band in dilute solutions of HDO in D_2O. Walrafen (18) states that

this behavior indicates that, "The ClO_4^- ion produces an extensive breakdown of the hydrogen-bonded water structure similar to the breakdown resulting from a large temperature rise . . . the ClO_4^- ion does not form directed hydrogen-bonds with water, in contrast to structure-breaking ions such as Cl^- and Br^- which form linear or nearly linear hydrogen-bonds with water." On the other hand, Brink and Falk (19) interpret the high-frequency component of the uncoupled O-H stretching band as due to O-H groups (they worked with HDO in D_2O) involved in weak hydrogen-bonds with the ClO_4^- ion. Their reason for this belief is that the frequency for this component is the same as the freqency for the O-H stretch for water in the hydrated crystals of the salts used. They interpret the low-frequency component as due to the O-H groups which are not associated with the anion. Furthermore, they believe that other ions such as NO_3^- and Cl^- do not result in components that can be spectroscopically resolved because the range of strengths of the anion-water interactions for these anions too closely overlap the range of strengths of water-water interactions.

If as Walrafen suggests (18) both the ClO_4^- and the Cl^- ions are water structure breakers but that Cl^- forms hydrogen-bonds with water and ClO_4^- does not, it might be expected that $\overline{C}_{p1}$ in dilute Cl^- solutions would be greater than $\overline{C}_{p1}$ for ClO_4^- solutions since there would be hydrogen-bonds

between water and the Cl^- ions to break with an increase in temperature. This is not the case and in fact $\bar{C}_{pl}$ for the ClO_4^- solutions is greater than $\bar{C}_{pl}$ for both the NO_3^- and Cl^- solutions up to concentrations of three molal where ion-ion interactions are becoming important. Therefore, it appears that the ClO_4^- ion plays a more complicated role in solution than just the role of a structure-breaker. What this role is and how it may be related to the weak interaction between the ClO_4^- ion and water proposed by Brink and Falk (19) is subject to speculation.

VI. SUMMARY

The high heat capacity of pure liquid water is explained in terms of a configurational contribution from the hydrogen-bonded structure of water. The fact that $\overline{C}_{p2}$ values for dilute rare earth nitrate and perchlorate solutions are negative is considered due to the structure-breaking effect of the added ions and the resulting decrease in the configurational contribution to the heat capacity.

The Φ_{cp} data for the rare earth perchlorates indicate that the rare earths are divided into two series with different coordination numbers. The rare earths Sm, Gd, Tb, and Dy exhibit intermediate behavior and are assumed to exist in solution as equilibrium mixtures of the two coordination types. The Φ_{cp} data for concentrated solutions indicate that the light rare earths La, Pr, and Nd also exhibit some tendency to exist in these solutions with a lower coordination number. No evidence is seen in the partial molal heat capacity data for the formation of inner-sphere complexes of the perchlorate ion with the rare earth ions.

The two series effect is not observed in the Φ_{cp} data for the rare earth nitrates. This is explained as due to the formation of inner-sphere complexes between the nitrate ion and the rare earth ions. In dilute solutions, data for $\overline{C}_{p1}$ across the rare earth series can be correlated with the trend in stability constants of rare earth mononitrate

complexes. In concentrated solutions the trend of $\overline{C}_{pl}$ across the series indicate the heavy rare earths are complexing more than the light rare earths.

For any given rare earth, $\overline{C}_{pl}$ values for the perchlorate solutions are greater than those for the nitrate and chloride solutions up to at least three molal. This may be due to a unique interaction between the perchlorate ion and water.

It should be emphasized that the arguments used in the discussion were of a very qualitative nature, and that more information about the interactions in solution is needed before quantitative interpretations can be made.

VII. BIBLIOGRAPHY

1. Arrhenius, S., Z. physik. Chem., 1, 631 (1887).

2. van't Hoff, J. H., Z. physik. Chem., 1, 481 (1887).

3. Milner, R., Phil. Mag., Ser. 6, 23, 551 (1912).

4. Debye, P. and E. Hückel, Physikal. Z., 24, 135 (1923). Original not available; cited in Onsager, L. and R. M. Fuoss, J. Phys. Chem., 36, 2689 (1932).

5. Harned, H. S. and B. B. Owen, "The Physical Chemistry of Electrolytic Solutions", 3rd. ed., Reinhold Publishing Corporation, New York, N.Y., 1958.

6. Fuoss, R. M. and L. Onsager, Proc. Natl. Acad. Sci. U.S., 47, 818 (1961).

7. Powell, J. E., "Separation of the Rare Earths by Ion Exchange". In Spedding, F. H. and A. H. Daane, eds., "The Rare Earths", pp. 55-73, John Wiley and Sons, Inc., New York, N.Y., 1961.

8. Templeton, D. H. and C. H. Dauben, J. Am. Chem. Soc., 76, 5237 (1954).

9. Ayers, B. O., "Apparent Molal Volumes of Some Rare Earth Salts in Aqueous Solution", unpublished Ph.D. thesis, Library, Iowa State University, Ames, Iowa, 1954.

10. Pikal, M. J. and F. H. Spedding, U.S. Atomic Energy Commission Report IS-1344 (Iowa State University, Ames, Iowa, Institute for Atomic Research) (1965).

11. Cullen, P. F., "Apparent Molal Volumes of Some Dilute Aqueous Rare Earth Salt Solutions at 25°C", unpublished Ph.D. thesis, Library, Iowa State University, Ames, Iowa, 1969.

12. DeKock, C. W., "Heats of Dilution of Some Aqueous Rare Earth Chloride Solutions at 25°C", unpublished Ph.D. thesis, Library, Iowa State University, Ames, Iowa, 1965.

13. Pepple, G. W., "Relative Apparent Molal Heat Contents of Some Aqueous Rare Earth Chloride Solutions at 25°C", unpublished Ph.D. thesis, Library, Iowa State University, Ames, Iowa, 1967.

14. Spedding, F. H. and K. C. Jones, J. Phys. Chem., 70, 2450 (1966).

15. Jones, K. C. and F. H. Spedding, U.S. Atomic Energy Commission Report IS-1355 (Iowa State University, Ames, Iowa, Institute for Atomic Research) (1965).

16. Walters, J. P. and F. H. Spedding, U.S. Atomic Energy Commission Report IS-1988 (Iowa State University, Ames, Iowa, Institute for Atomic Research) (1968).

17. Dryjanski, Piotr and Z. Kecki, Rocz. Chem., 43, 1053 (1969).

18. Walrafen, G. E., J. Chem. Phys., 52, 4176 (1970).

19. Brink, G. and M. Falk, Can. J. Chem., 48, 3019 (1970).

20. McCabe, W. C., S. Subramanian and H. F. Fisher, J. Phys. Chem., 74, 4360 (1970).

21. Mohs, M. A., "Relative Apparent Molal Heat Contents of Some Aqueous Rare Earth Salt Solutions at 25°C", unpublished Ph.D. thesis, Library, Iowa State University, Ames, Iowa, 1970.

22. Spedding, F. H. and C. F. Miller, J. Am. Chem. Soc., 74, 3158 (1952).

23. Korbl, J. and R. Pribil, The Chemist Analyst, 45, 102 (1956).

24. Osborne, D. W. and L. Stein, Ann. Rev. Phys. Chem., 13, 127 (1962).

25. Sturtevant, J. M., "Calorimetry", chapter 10 in "Physical Methods of Organic Chemistry", 3rd ed., Vol. 1, ed. A. Weissberger, Interscience Publishers, Inc., New York, N.Y., 1959.

26. Rossini, F. D., "Experimental Thermochemistry", Interscience Publishers, Inc., New York, N.Y., 1956.

27. Skinner, H. A., "Experimental Thermochemistry", Vol. 2, Interscience Publishers, Inc., New York, N.Y., 1962.

28. Swietoslawski, W.,"Microcalorimetry", Reinhold Publishing Corporation, New York, N.Y., 1946.

29. Armstrong, G. T., J. Chem. Ed., 41, 297 (1964).

30. Osborne, N. S., H. F. Stimson and D. C. Ginnings, National Bureau of Standards Journal of Research, 23, 197 (1939).

31. Hoge, H. J., National Bureau of Standards Journal of Research, 36, 111 (1946).

32. Randall, M. and F. D. Rossini, J. Am. Chem. Soc., 51, 323 (1929).

33. Epikin, Yu. A. and M. S. Stakhanova, Zh. Fiz. Khim., 41, 2148 (1967).

34. Worthing, A. G. and J. Geffner, "Treatment of Experimental Data", John Wiley and Sons, Inc., New York, N.Y., 1943.

35. Eisenberg, D. and W. Kauzmann, "The Structure and Properties of Water", Oxford University Press, New York, N.Y., 1969.

36. Holtzer, A. and M. F. Emerson, J. Phys. Chem., 73, 26 (1969).

37. Karraker, D. G., Inorg. Chem., 7, 473 (1968).

38. Morgan, L. O., J. Chem. Phys., 38, 2788 (1963).

39. Karraker, D. G., J. Chem. Ed., 47, 424 (1970).

40. Moeller, T., D. F. Martin, L. C. Thompson, R. Ferrus, G. R. Feistel and W. J. Randall, Chem. Rev., 65, 1 (1965).

41. Niedzielski, R. J. and J. C. Horvath, J. Inorg. Nucl. Chem., 30, 1272 (1968).

42. Forsberg, J. H. and T. Moeller, Inorg. Chem., 8, 883 (1969).

43. Karraker, D. G., J. Inorg. Nucl. Chem., 33, 479 (1971).

44. Spedding, F. H., M. J. Pikal and B. O. Ayers, J. Phys. Chem., 70, 2440 (1966).

45. Nakamura, K. and K. Kawamura, Bulletin of the Chemical Society of Japan, 44, 330 (1971).

46. Hester, R. E. and R. A. Plane, Inorg. Chem., 3, 769 (1964).

47. Sutcliffe, L. H. and J. R. Weber, Trans. Faraday Soc., 52, 1225 (1956).

48. Alei, M., Jr., Inorg. Chem., 3, 44 (1964).

49. Peppard, D. F., G. W. Mason and I. Hucher, J. Inorg. Nucl. Chem., 24, 881 (1962).

50. Abrahamer, I. and Y. Marcus, J. Inorg. Nucl. Chem., 30, 1563 (1968).

51. Choppin, G. R. and W. F. Strazik, Inorg. Chem., 4, 1250 (1965).

52. Frank, H. S. and M. Evans, J. Chem. Phys., 13, 507 (1945).

53. Bukietynska, K. and G. R. Choppin, J. Chem. Phys., 52, 2875 (1970).

54. Reuben, J. and D. Fiat, J. Chem. Phys., 51, 4909 (1969).

55. Knoeck, J., Anal. Chem., 41, 2069 (1969).

56. Abrahamer, I. and A. Marcus, Inorg. Chem., 6, 2103 (1967).

57. Rumanova, I. M., G. F. Volodina and N. V. Belov, Crystallography, 9, 545 (1965), translated edition of Kristallografiya, 9, 624 (1964).

58. Nelson, D. L. and D. E. Irish, J. Chem. Phys., 54, 4479 (1971).

59. Anagnostopoulos, A. and P. O. Sakellaridis, J. Inorg. Nucl. Chem., 32, 1740 (1970).

60. Coward, N. A. and R. W. Kiser, J. Phys. Chem., 70, 213 (1966).

61. Peppard, D. F., J. P. Faris, P. R. Gray and G. W. Mason, J. Phys. Chem., 57, 294 (1953).

62. Peppard, D. F., W. J. Driscoll, R. J. Sironen and S. McCarty, J. Inorg. Nucl. Chem., 4, 326 (1957).

63. Klygin, A. E., I. D. Smirnova, N. S. Kolyada, E. N. Malkina, A. M. Gertseva, V. A. Lekae and D. M. Zarvazhnova, Zh. Neorg. Khim., 15, 622 (1970).

64. Ferrer, P., Thesis, Madrid (1950). Original not available; cited in Parker, V. B., U.S. Department of Commerce Report, NSRDS-NBS-2, 5, (1965).

65. Herzberg, G., "Molecular Spectra and Molecular Structure", Vol. 2, D. Van Nostrand Company, Inc., New York, N.Y., 1945.

66. Wall, T. T. and D. F. Hornig, J. Chem. Phys., 43, 2079 (1965).

67. Walrafen, G. E., J. Chem. Phys., 48, 244 (1968).

68. Senior, W. A. and R. E. Verrall, J. Phys. Chem., 73, 4242 (1969).

VIII. ACKNOWLEDGEMENTS

The author wishes to express his appreciation to Dr. F. H. Spedding for his patience and guidance throughout the course of this research and in the preparation of this thesis. The author also wishes to extend his appreciation to his wife, Margery, for her encouragement throughout his graduate work and for the typing of this thesis. In addition, thanks are extended to the author's associates for their cooperation and assistance during the course of this work.